Department of Electrical Engineering

University of Adelaide

# SWITCH DIVERSITY SYSTEM IN MOBILE RADIO

submitted for

the degree of

Master of Engineering Science

THE UNIVERSITY OF ADELAIDE

This thesis embodies the results of supervised project work which made up All of the work for the degree.

Van Van Vu

ACKNOWLEDGEMENTS

I would like to thank my supervisor, Dr. B.R. Davis, for his assistance and supervision of this thesis. I also wish to thank the University of Adelaide for offering me a University Research Grant to carry out my studies.

CONTENTS

## SUMMARY

In the past few years, various techniques of space diversity have been studied to provide an increase in quality of communication in Mobile Radio. When the noise inputs on the diversity branches are highly correlated, switch diversity systems offer an attractive, economical alternative to the well-known diversity techniques, which are selection, maximal-ratio, and equal-gain combining. A data communication system, using Frequency-Shift-Keying (FSK) and switch diversity, is investigated, when the transmission is subject to Rayleigh fading as encountered in Mobile Radio.

Mobile Radio propagation and principles of diversity reception and techniques are first reviewed, and then switch diversity is studied. Error rates are calculated for a receiver using switch diversity and non-coherent FSK demodulator. An experimental receiver was constructed in the laboratory. The experimental results, obtained by using two simulated independently Rayleigh fading signals, agree reasonably well with the theoretical predictions. They show a power saving of about 7 db at reasonable error rates (from $10^{-3}$ to $10^{-4}$).

STATEMENT OF ORIGINALITY.

This thesis contains no material which has been accepted for the award to me of any degree or diploma in any University and, to the best of my knowledge and belief, the thesis contains no material previously published or written by another person except where due reference is made in the text of the thesis.

## List of Symbols

| | |
|---|---|
| $r$, $r_1$, $r_2$ | received signal envelopes |
| $R$ | switch-diversity resultant signal envelope |
| $b_o$ | signal power, $2b_o = \langle r^2 \rangle$ |
| $f_c$ | carrier frequency in Hz |
| $v$ | speed of vehicle in m/sec |
| $\lambda$ | wavelength in m, $\lambda = \frac{c}{f_c}$ |
| $c$ | speed of light in m/sec |
| $f_m$ | maximum Doppler shift, $f_m = \frac{v}{\lambda}$ |
| $\gamma$ | local (averaged over one RF cycle) mean carrier-to-noise power ratio CNR |
| $\gamma_o$ | mean CNR over fading, $\gamma_o = \langle \gamma \rangle$ |
| $T$ | switching threshold |
| $p$ | probability of a successful switching |
| $q$ | probability of an unsuccessful switching |
| $\tau_p$ | average duration when the signal envelope is above T |
| $\tau_q$ | average duration of a fade below T |

# CHAPTER I

## INTRODUCTION

In the Mobile Radio situation, the line-of-sight is usually obstructed by buildings and terrain. The propagation is via many scattering paths, each with different propagation time delay due to reflections from, and diffractions around obstacles [1] - [2]. At a given point in the space, the received signal consists of many plane waves whose amplitudes, phases, and angles of arrival relative to the direction of vehicle motion are random [3]-[4]. These plane waves combine to produce a fluctuating signal strength, whose maxima are about half a wavelength apart. At 500 MHz, the spacing is about 30 cm. Thus as the mobile unit is moving, there are very rapid random fluctuations in the strength of the received signal at the mobile antenna. The base station also experiences the same fast fading as the mobile transmitter moves. In addition to the amplitude variations, the phase of the received signal also varies in a random way [4], the phase variations appear as a random FM in a receiver using FM discriminator.

In areas where there is no significant direct signal from the transmitter, the envelope of the received signal follows Rayleigh distribution in a small area, about a few tens of wavelengths, where the mean signal strength is approximately constant [3]-[6]. The mean signal

strength also varies because of the effects of the environment, and is found to have very nearly a log-normal distribution with a standard deviation between 5 and 10 db [4],[7].

If several signals received at the mobile unit or the base station are uncorrelated in space, frequency, or polarization, i.e. they do not have identical flucuations, it is very unlikely that they would enter a deep fade at the same time. Some suitable techniques which combine the signals would be very useful in reducing the effect of fading. The techniques are called "Diversity Techniques". The effect of random FM is also reduced or eliminated by the techniques used to combat fading [8]-[9]. The most well-known diversity technique is Space Diversity. In space diversity systems, the essential uncorrelation of the envelopes of the received signals derives from the mobile unit antennas whose separations are of the order of one-half wavelength or more [10]. Since the scatterers are close to mobile units, and the elevated base antennas are usually on a good site, the base antennas must be further apart to achieve the required decorrelation [11]. Separations in the order of tens of wavelengths are adequate at the base station.

The signal processing schemes which take advantage of the uncorrelated fading to reduce the effect of fading, are switch diversity, selection diversity, equal-gain diversity, and maximal-ratio diversity [8],[12]-[19].

The main object of this thesis is to present a study of switch space-diversity in Mobile Radio, and the reduction of the error probability in Frequency-Shift-Keying (FSK) system on the use of switch diversity in Mobile Radio environment. However, before this is done, some introductory background is given. Chapter II deals with the Mobile Radio reception, and the concept of diversity. In Chapter III, the most well-known diversity techniques are reviewed. Detailed studies of switch diversity are given in Chapter IV. Under conditions assumed to simplify the theoretical studies of the switch diversity technique, the distribution and density functions of the envelope of the resultant signal are derived, and then the average error probability for non-coherent FSK receiver is calculated.

In Chapter V, an experimental non-coherent FSK receiver using switch diversity is described. The error rates, under different conditions, are obtained to support the theoretical prediction. In the final chapter, some general comments are made about the receiver.

CHAPTER II

# MOBILE RADIO DIVERSITY

## *II.1 Mobile Radio Reception*

In the Mobile Radio situation, there is usually an elevated base station on a good site, linked with a number of vehicles at some distance away. Because of the natural and man-made obstacles, there is often no direct path between transmitter and receiver, the propagation is via scattering paths from those obstacles [1]-[2]. The received signal is the resultant of many coming plane waves whose amplitudes, phases, and angles of arrival relative to the direction of vehicle motion are random [3]-[4]. The incoming waves interfere and produce a signal strength pattern with maxima spaced approximately half a wavelength apart, as shown in Fig. 1 [4]. As the mobile station moves through the pattern, the received signal at the mobile antenna fades rapidly and deeply.

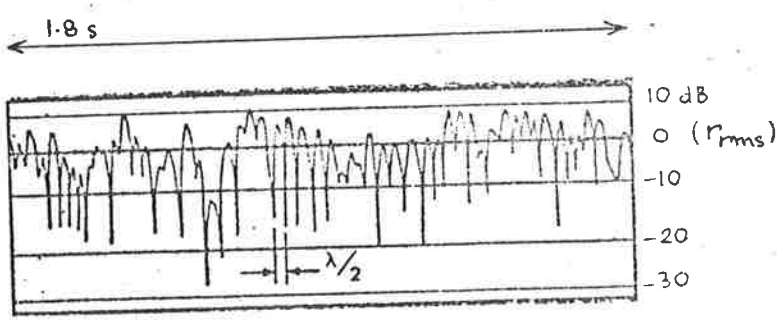


Fig. 1: Typical received signal at 836 MHz and 25 km/hr.

For a distance of a few tens wavelength where the mean signal strength is approximately constant, and there is no direct path between the transmitter and receiver, the experimental results have shown that the envelope of the received signal follows a Rayleigh distribution [3]-[7].

The probability density function of the signal envelope is given by

$$p(r) = \begin{cases} \frac{r}{b_o} \exp\left(-\frac{r^2}{2b_o}\right) & R \geq 0 \\ 0 & R < 0 \end{cases}$$

where $b_o$ = signal power

$2b_o = \langle r^2 \rangle = r^2_{rms}$

and the probability distribution function is

$$P[r \leq A] = \int_0^A p(r)\, dr$$

$$= 1 - \exp\left(-\frac{A^2}{2b_o}\right)$$

The function p(r) is presented in Fig. 2. The peak of p(r) occurs at

$$r = \sqrt{b_o}$$

$$= \frac{1}{\sqrt{2}} r_{rms}$$

The median (50 per cent cumulative distribution) point is found at

$$r = 1.185 \sqrt{b_o}$$

and the average value of r

$$\langle r \rangle = 1.25 \sqrt{b_o} = \sqrt{\frac{\pi}{2}} \sqrt{b_o}$$

The random multipath effect that yields a Rayleigh distributed received signal envelope lends to establish a simple physical model from which other properties of the received signal may be predicted [6],[20]. It seems reasonable on physical grounds to assume that the received signal is made up of a number of horizontally travelling plane waves with random amplitudes and angles of arrival. The phases of the waves are uniformly distributed from 0 to $2\pi$. The amplitudes and phases are also assumed to be independent. Clarke [6] uses the proposed model, where the received signal is approximated by narrow-band Gaussian noise, to predict the Rayleigh distribution of the received signal envelope. He derived the signal amplitude spectrum and the spatial correlation functions of the envelopes of the electric and magnetic fields at the mobile antenna.

*(a) Correlation Coefficients*

Using the expression of the received signal as a sum of incident plane waves, Clarke [6] obtained correlation coefficients of the field components. The correlation coefficient of the electric field is given by

$$\rho_E = J_o^2 (kd)$$

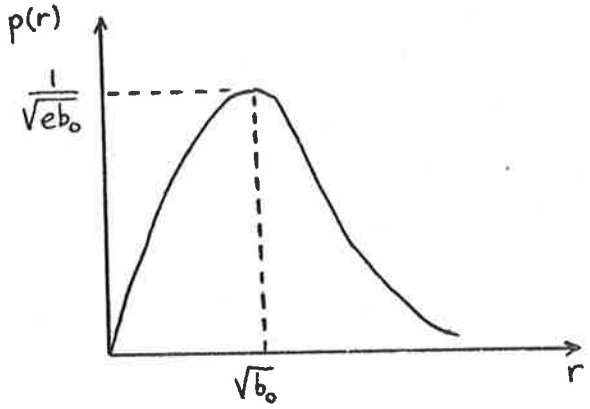


$$p(r) = \frac{r}{b_o} \exp\left(-\frac{r^2}{2b_o}\right)$$

$$\langle r^2 \rangle = 2b_o$$

$$\langle r \rangle = \sqrt{\frac{\pi}{2}}\sqrt{b_o}$$

Fig. 2: Rayleigh probability density function

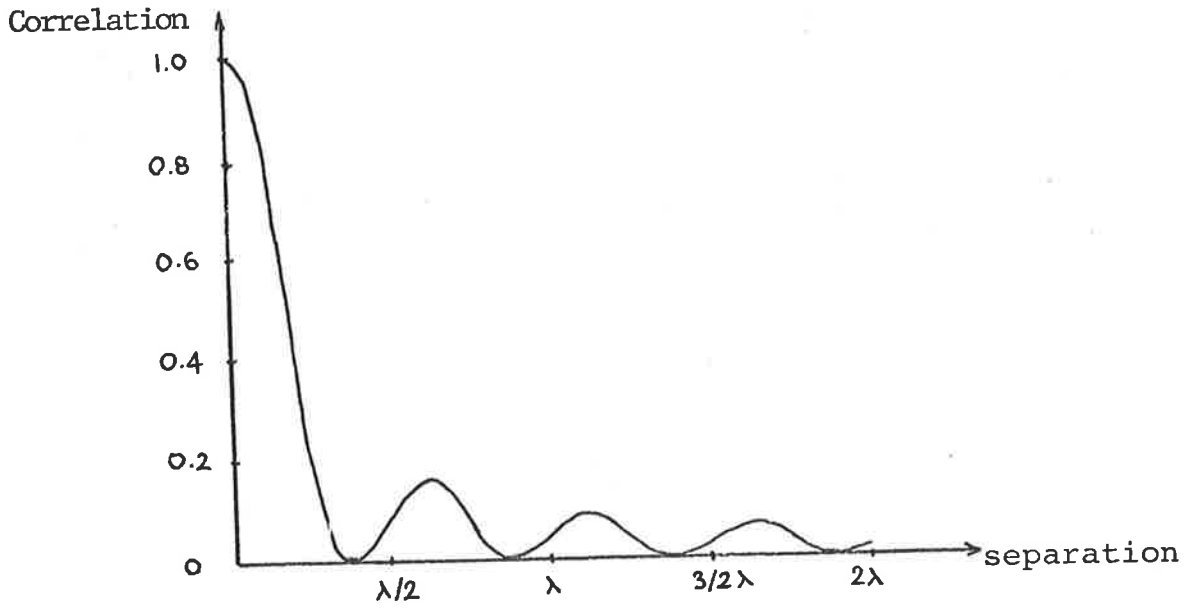


Fig. 3: Correlation coefficient of the received signal envelope.

where $J_o$ is the zero-order Bessel function of the first kind

$k = \frac{2\pi}{\lambda}$ (free-space phase constant)

$d$ = spatial separation

$\rho_E$ is plotted in Fig. 3.

He also showed that all three field components are uncorrelated at zero separation.

*(b) Signal Spectrum*

Assuming that the scattered set of the incoming waves is uniformly distributed angularly, i.e. the probability density function $p(\alpha) = \frac{1}{2\pi}$, where $\alpha$ is the arrival angle relative to the direction of vehicle motion, the received signal amplitude spectrum is determined by the vehicle speed and antenna pattern [6].

For a mobile unit travelling at a speed v with a vertical monopole antenna, the spectrum is given by

$$S(f) = \frac{2b_o}{\pi f_m} \left[1 - \left(\frac{f-f_c}{f_m}\right)^2\right]^{-\frac{1}{2}} \qquad |f-f_c| \leq f_m$$

where $f_m = \frac{v}{\lambda}$, the maximum Doppler shift

$f_c$ is the carrier frequency.

The spectrum of the received signal after envelope defection is given by [6].

$$S_{baseband} = K\left[1 - \left(\frac{f}{f_m}\right)^2\right]^{-\frac{1}{2}} \qquad |f| \leq 2f_m$$

The spectrum rises gradually toward zero frequency and has a sharp cut-off at twice the maximum Doppler shift. There is a good agreement between the experimental spectrum obtained by Rustako [18] and the theoretical one.

*(c) Level Crossing Rate*

One of the interesting features of the received signal is the expected rate N(A) at which the received signal envelope r falls below a specified signal level A, i.e. the rate at which the envelope crosses the level r = A with positive slope. The level crossing rate N(A) is given by [21]

$$N(A) = \int_0^\infty \dot{r}\, p(A,\dot{r})\, d\dot{r}$$

where $p(A,\dot{r})$ is the joint density function of r and $\dot{r}$ (time derivative of r) at r = A

$$p(r,\dot{r}) = \int_0^{2\pi} d\theta \int_{-\infty}^{+\infty} p(r,\dot{r},\theta,\dot{\theta})\, d\dot{\theta}$$

where [21]

$$p(r,\dot{r},\theta,\dot{\theta}) = \frac{r^2}{4\pi^2 b_o b_2} \exp\left[-\tfrac{1}{2}\left(\frac{r^2}{b_o} + \frac{\dot{r}^2}{b_2} + \frac{r^2\dot{\theta}^2}{b_2}\right)\right]$$

$$b_2 = (2\pi)^2 \int_{f_c-f_m}^{f_c+f_m} S(f)\,(f - f_c)^2\, df$$

$$= (2\pi)^2 \tfrac{1}{2} f_m^2\, b_o$$

for vertical monopole antenna.

Therefore

$$p(r,\dot{r}) = \frac{r}{b_o} \exp\left(-\frac{r^2}{2b_o}\right) \frac{1}{\sqrt{2\pi b_2}} \exp\left(-\frac{\dot{r}^2}{2b_2}\right)$$

Substituting in the above expression of the level crossing rate

$$N(A) = \sqrt{\frac{b_2}{2\pi b_o}} \frac{A}{b_o} \exp\left(-\frac{A^2}{2b_o}\right)$$

For a vertical monopole antenna, the level crossing rate is given by

$$N(A) = \sqrt{\frac{\pi}{b_o}} f_m A \exp\left(-\frac{A^2}{2b_o}\right)$$

and is presented in Fig. 4.

The maximum crossing rate occurs at the signal level -3 db relative to $r_{rms}$. At 500 MHz, and vehicle speed of 90 km/hr, the received signal crosses the -10 db level at the rate of 30 times/sec approximately.

*(d) Average Duration of Fade*

The level crossing rate N(A) can be written as

$$N(A) = \frac{\text{probability that } r < A \text{ in one second } p[r \leq A]}{\text{average duration of fade below A, } t(A)}$$

Therefore

$$t(A) = \frac{p[r \leq A]}{N(A)}$$

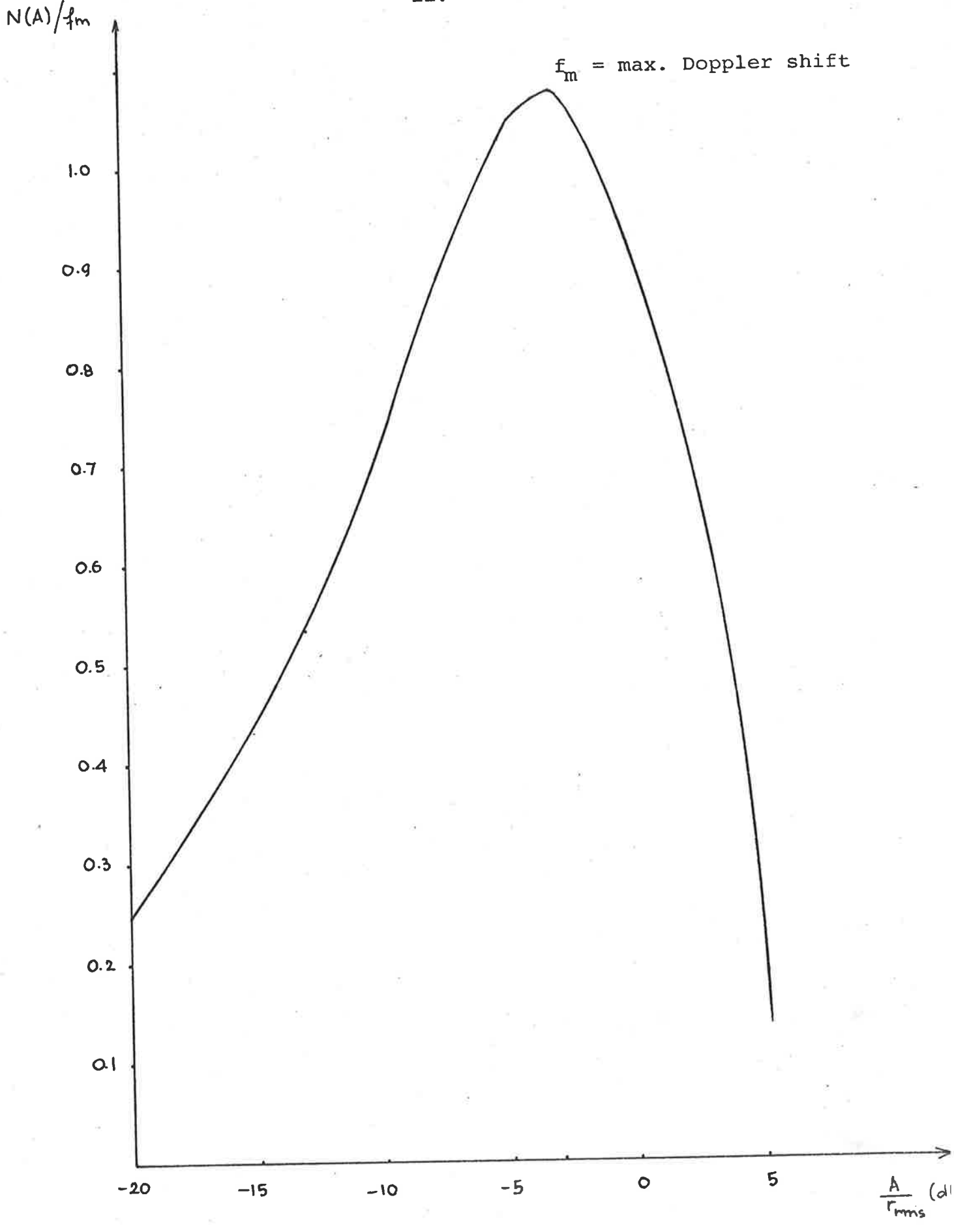


Fig. 4: Level crossing rate for a vertical monopole antenna.

$$= \sqrt{\frac{b_o}{\pi}} \; \frac{1}{f_m A} \left[ \exp\left( + \frac{A^2}{2b_o} \right) - 1 \right]$$

for a vertical monopole.

t(A) is plotted in Fig. 5. The average duration of a -10 db fade relative to $r_{rms}$ at 500 MHz and 90 km/hr is about 3 msec.

*(e) Coherence Bandwidth*

The coherence bandwidth of a channel is defined as the maximum width of the band in which the statistical properties of two signals are strongly correlated.

To be definite, let us define the coherence bandwidth as the bandwidth within which fading has 0.9 or greater correlation. The experimental results have shown that the coherence bandwidth can be as low as 40 KHz in urban areas, and as large as 250 KHz in suburban areas [22].

The coherence bandwidth is related to the time delay spread, and is approximately inversely proportional to the standard deviation of the time delays [20].

To obtain non-selective fading, the transmission bandwidths have to be smaller than the coherence bandwidths.

*(f) Random FM*

The phase variation of the received signal appears as a random FM at the output of an FM discriminator. Random

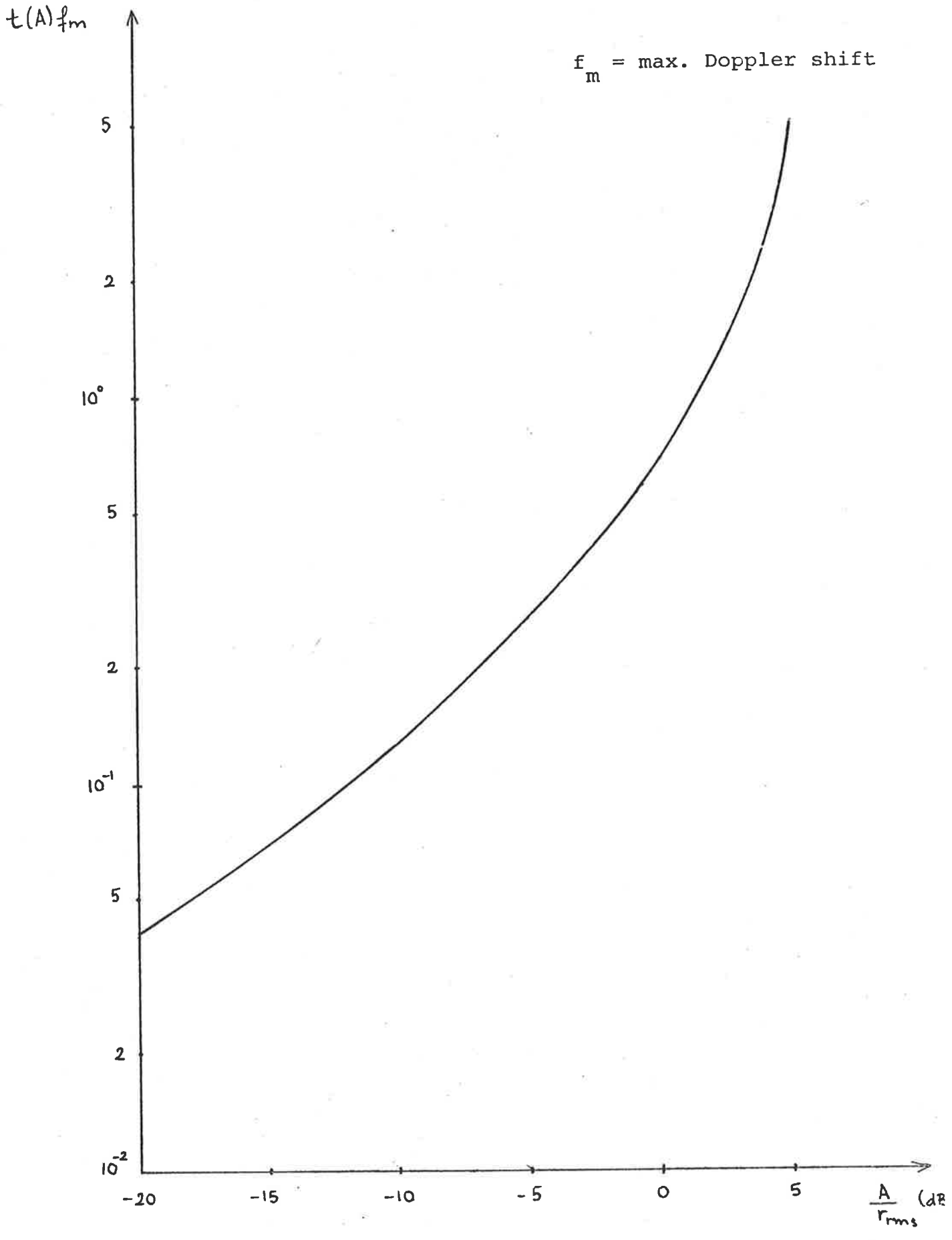


Fig. 5: Average duration of fade for a vertical monopole.

FM introduces additional noise in FM systems. The spectrum of random FM extends from zero to about twice the maximum Doppler shift. Above this value, the spectrum falls at 1/f [20]. The noise due to random FM imposes an upper limit on baseband SNR for FM systems, and it is independent of the transmitted signal power.

Davis [23] calculated the maximum achievable SNR in voice transmission (300 Hz - 3000 Hz baseband bandwidth) for a mobile unit with a vertical monopole antenna

$$SNR_{max} = \frac{W^2(\alpha-1)^2}{10\sigma_D^2 \ln 10}$$

where $W$ = 3000 Hz

$\alpha$ = peak frequency deviation

$\sigma_D$ = radius of gyration of the Doppler spectrum

$= \frac{f_m}{\sqrt{2}}$

At 900 MHz and 96 km/hr, the maximum SNR's are given below for various values of $\alpha$.

| $\alpha$ = | 2 | 3 | 4 | 6 | 8 | 10 | 15 | 20 |
|---|---|---|---|---|---|---|---|---|
| $SNR_{max}$ db | 20.8 | 26.8 | 30.3 | 34.8 | 37.7 | 39.9 | 43.7 | 46.4 |

Random FM limits the quality of voice transmission for low $\alpha$ even at infinite average CNR. The effect of random FM can be reduced or eliminated by diversity techniques, used to combat fading [9].

*II.2 Diversity Concepts in Mobile Radio*

In Mobile Radio, where the received signal is subject to fading, the reception can be improved if two or more signals are available, and they fade independently since the probability of simultaneous fades of two or more signals is less than that of fading of one signal alone. For example, if two independently Rayleigh fading signals are obtained, the probability of simultaneous fades of more than 20 db, relative to the rms signal amplitude, is 0.01% whereas it is 1% for each received signal. If the receiver input is derived from the stronger of two signals at any instant (selection diversity), the probability of fades for different signal levels is shown in Fig. 6.

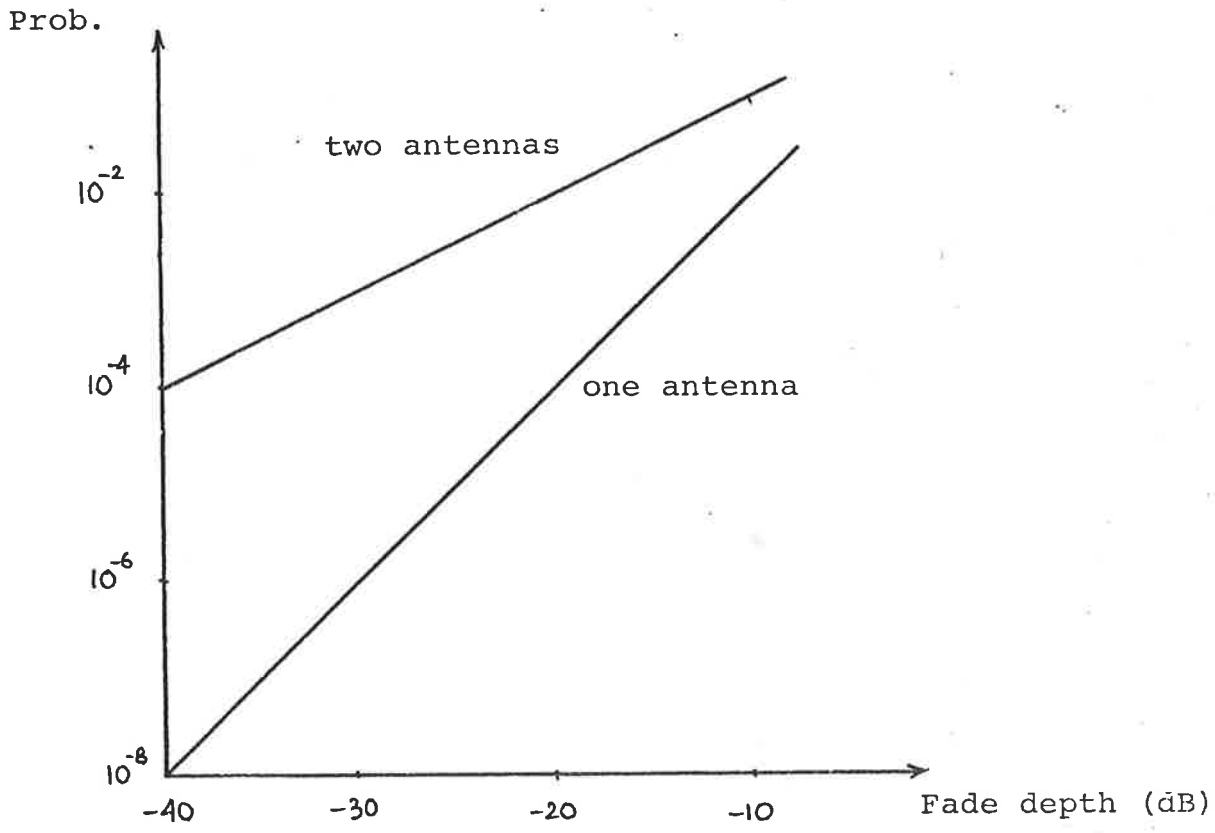


Fig. 6: Probability of fades for different fade depth.

The improvement can also be made by some suitable combination of the received signals. The combining methods involve simple weighted linear sums of the received signals [12]. In the literature, these methods are commonly identified as

(i) switch diversity

(ii) selection diversity

(iii) maximal-ratio diversity

(iv) equal-gain diversity.

In the next chapter, these diversity techniques will be briefly reviewed.

In this section, methods for achieving independently fading signals in Mobile Radio will be discussed, and the effect of correlation between diversity branches on the resultant signal will also be briefly considered.

*(a) Space Diversity*

At the mobile unit, the distance between maxima of the received signal strength is about half a wavelength apart. If the signals were received from antennas separated by half a wavelength or so, they would not have identical fluctuations, and independently fading signals could, therefore, be obtained. This can be seen from the correlation coefficient of the signal envelopes at two vertical monopole antennas d apart on the moving mobile unit [6].

$$\rho(d) = J_o^2 (kd)$$

$\rho(d)$ is shown in Fig. 3. For antennas spaced 1/4, 3/4, and 5/4 wavelength apart, the correlation coefficients of the signal envelopes at the antenna terminals are about 0.25, 0.06, and 0.03, respectively. Staras [24] and Packard [25] showed that at these values of correlation coefficient, the advantage of diversity is negligibly impaired.

Space diversity can be used also at the base station. However, as the scatterers are mainly in the vicinity of the mobile and the elevated base station antennas are on a good site, the base antennas must be considerably further apart to achieve uncorrelated signals [11]. The correlation coefficient of less than 0.7 between received signals can be tolerated [12], and to get a correlation of 0.7, the antenna spacing at the base station varies from 25$\lambda$ to 80$\lambda$, depending on the direction of the coming signals relative to the axis of the antennas.

*(b) Frequency Diversity*

Independent fading can also be obtained if the same signal is transmitted at carrier frequencies whose separations are larger than the coherence bandwidth.

The frequency diversity reception is possible, but because of the multiple frequency allocation, the need for transmitting and combining signals at different frequencies, this is not a practical proposition.

*(c) Polarization Diversity*

Two-branch diversity system, using polarization diversity in Mobile Radio, is also possible [26]. At the base station, there are a vertically polarized (VP) and a horizontally polarized (HP) antenna. At the mobile unit, both VP and HP antennas are also required. It was shown that the fadings of two branches are Rayleigh distributed, and the correlation between them is less than 0.2, with no restriction on antenna spacings both at the mobile and at the base.

*(d) Time Diversity*

Time diversity is applied only to data transmissions. In time diversity systems, the same bit of information is transmitted through the same channel more than once at time intervals greater than the reciprocal of the fading rate, and the appropriate combination of the repetitions will give a diversity performance [27].

Time diversity systems do not find favour because they reduce the traffic capacity and require information storage.

CHAPTER III

# SPACE-DIVERSITY SYSTEMS IN MOBILE RADIO

There are four main types of diversity combining, taking advantage of uncorrelated fading, to reduce the effect of fading in Mobile Radio

1. Selection diversity
2. Switch diversity
3. Maximal-Ratio diversity
4. Equal-Gain diversity.

These combining techniques will be briefly described in this chapter to illustrate their principles of operation and performance.

It should be pointed out that these diversity techniques can not compensate the variations of the mean signal strength, due to the environment. Only short-term fading is considered in the mathematical model, used to study diversity performance.

When reception involves linear modulation, it is irrelevant whether the signals are combined before or after demodulation. However in the case of FM or other non-linear demodulation, the performance difference between postdetection and predetection diversity combining will arise. This matter will be discussed later.

In all the work, it is assumed that the signals on all diversity branches are independent and Rayleigh-distributed with equal mean carrier-to-noise power ratio (CNR) $\gamma_o$ over short-term fading.

The density function of the signal envelope $r_i(t)$ is

$$p(r_i) = \begin{cases} \frac{r_i}{b_o} \exp\left(-\frac{r_i^2}{2b_o}\right) & r_i \geq 0 \\ 0 & r_i < 0 \end{cases}$$

where $\langle r_i^2 \rangle = 2b_o$

$= 2 \times$ (mean signal power)

The CNR $\gamma_i$ per branch is

$$\gamma_i = \frac{r_i^2}{2N}$$

$\frac{r_i^2}{2}$ = local (averaged over one RF cycle) mean signal power per branch

$N$ = mean noise power per branch.

Then $\gamma_i$ has the probability density function

$$p(\gamma_i) = \frac{1}{\gamma_o} \exp\left(-\frac{\gamma_i}{\gamma_o}\right)$$

where $\gamma_o = \langle \gamma_i \rangle = \frac{b_o}{N}$ .

## *III.1 Diversity Techniques*

### *(a) Selection Diversity*

A postdetection selection diversity receiver contains a number of separate receivers, as shown in Fig. 7. A decision circuit continuously samples all the receiver outputs and selects the one having the highest baseband SNR to pass onto the listener.

As far as the statistics of the output signal are concerned, it is unimportant whether the selection is done at baseband, IF or RF. However, in an FM system, where the selection is done before frequency detection, there is switching transient noise due to the fact that the diversity branches are not in phase.

The distribution of the CNR $\gamma$ of the resultant signal is given by [27]

$$P_M(\gamma) = [1 - \exp(-\frac{\gamma}{\gamma_o})]^M$$

where M is the number of diversity branches.

$P_M(\gamma)$ is plotted in Fig. 8 for M = 1, 2, 3, 4 and 6. It shows for the same reliability level, the signal power savings offered by selection diversity. For example, at 90% reliability level, the power saving offered by 2-branch is 10 db.

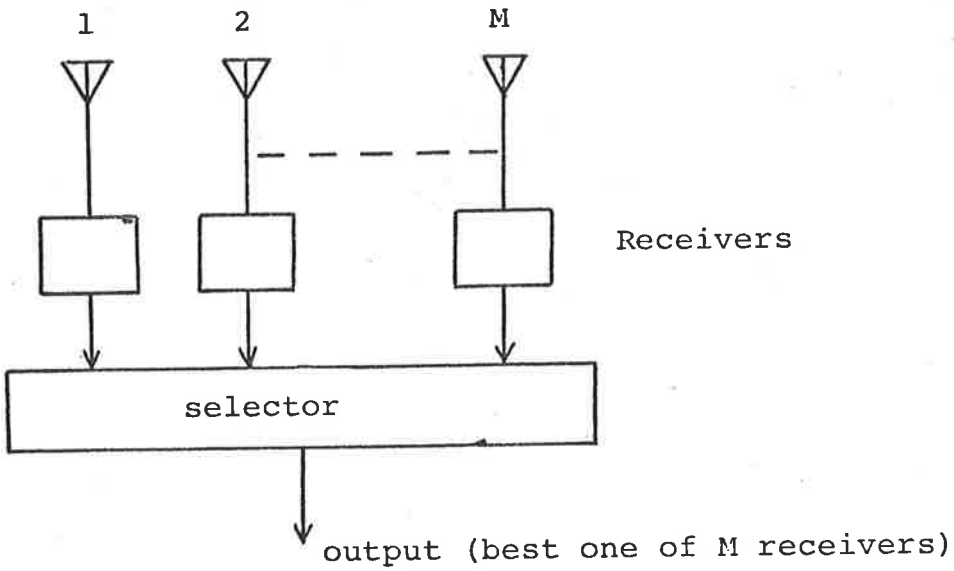


Fig. 7: Principle of a predetection selection diversity receiver.

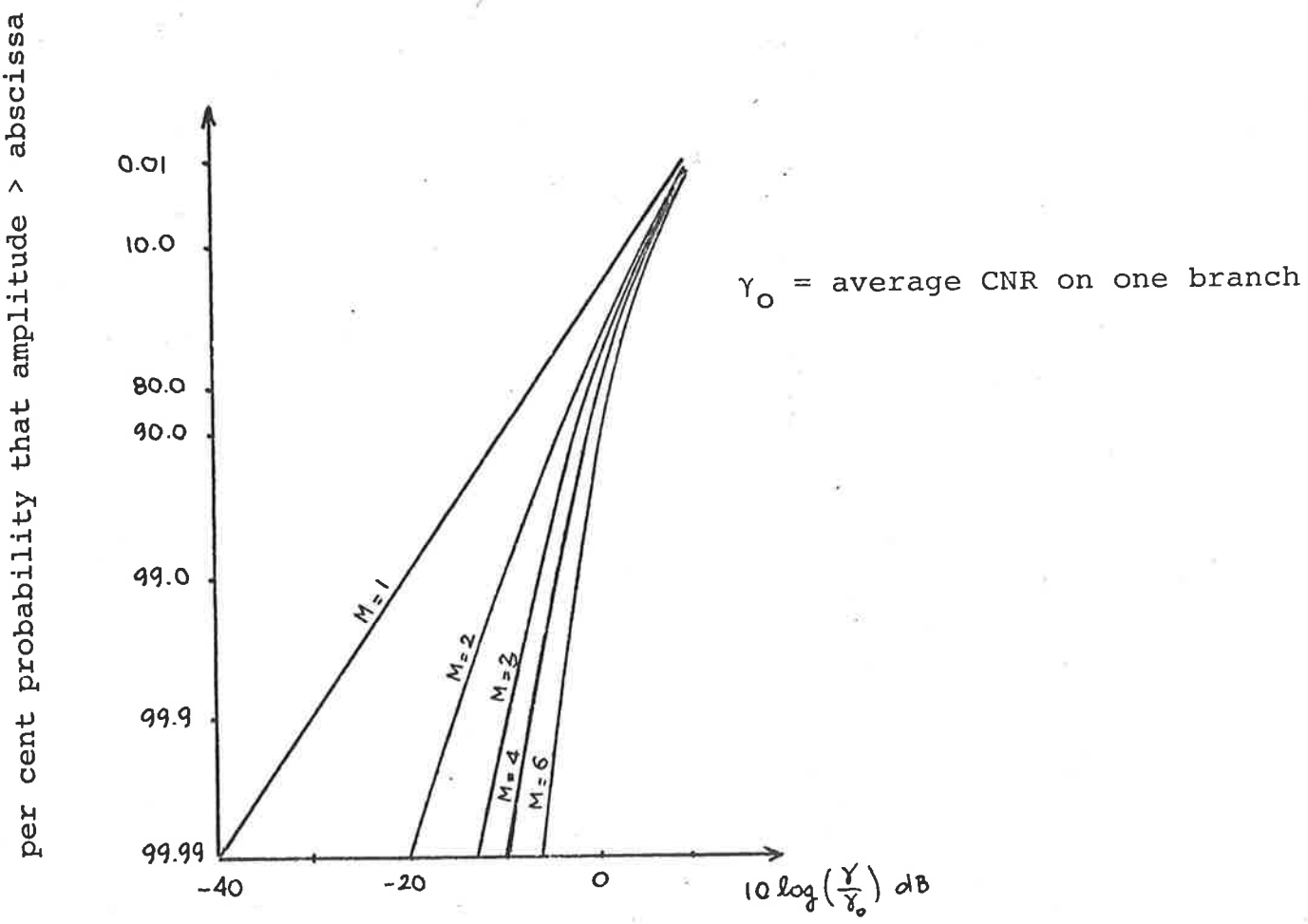


Fig. 8: Probability distribution of CNR $\gamma$ for M-branch selection diversity system.

The density function of $\gamma$ is

$$p_M(\gamma) = \frac{d}{d\gamma} P_M(\gamma) = \frac{M}{\gamma_o} \left[1 - \exp\left(-\frac{\gamma}{\gamma_o}\right)\right]^{M-1} \exp\left(-\frac{\gamma}{\gamma_o}\right)$$

This gives the mean CNR $\bar{\gamma}$ of the resultant signal

$$\bar{\gamma} = \int_o^\infty \gamma\, p_M(\gamma)\, d\gamma$$

$$= \gamma_o \sum_{i=1}^{M} \frac{1}{i}$$

This means that increasing M beyond 2 or 3 is not very profitable. This fact is also clearly demonstrated by the distribution curves.

*(b) Switch Diversity*

Switch diversity is a modified selection diversity. A switch diversity receiver uses only one receiver which is connected to one of two separate antennas by a switch, as shown in Fig. 9. If the signal in use falls below a predetermined threshold, the receiver is switched to the other antenna. The receiver performance will be studied in detail in the next chapter.

The switching can be done at the base station. The mobile-to-base path is used as a signalling channel in addition to carrying information. The base transmitter is connected to one of its two antennas. Whenever the signal, received at the mobile unit falls below the

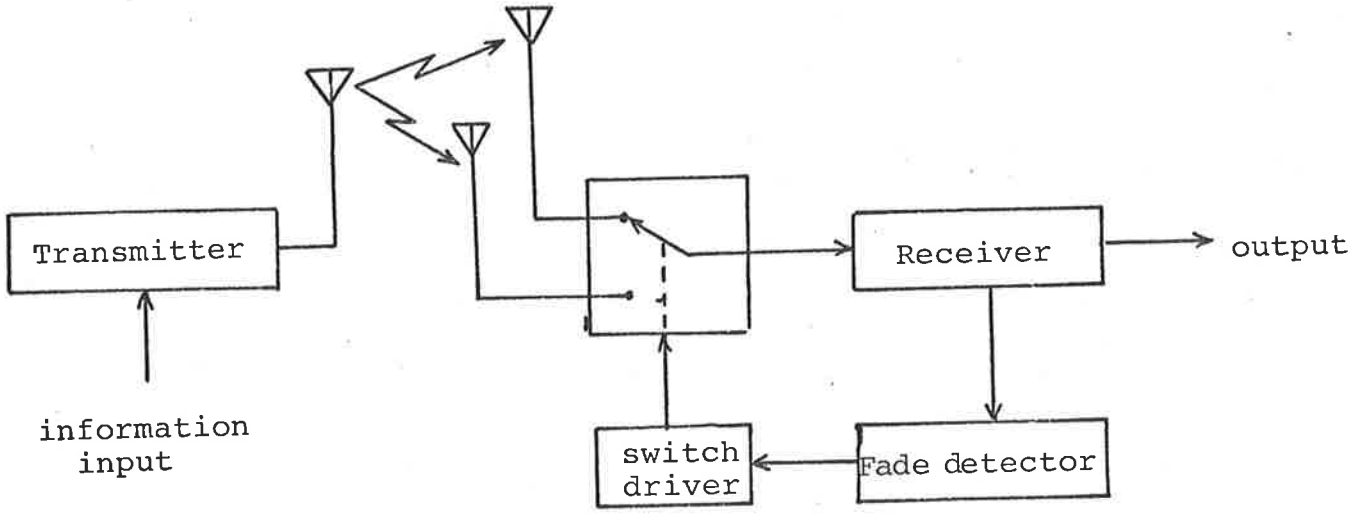


Fig. 9: Principle of a switch diversity system.

switching threshold, it signals the base station, and the transmitter is switched to the other antenna.

*(c) Maximal-Ratio Diversity*

This is a more sophisticated diversity method where all the received signals are combined in such a way that the CNR of the resultant signal has the achievable maximum value, which is the sum of all individual CNR's. It is obvious that the Maximal-Ratio diversity offers the best reduction of fading. But this can be only achieved if the conditions of locally uncorrelated noise and locally-coherent signals are satisfied [12].

Fig. 10 shows a simplified block diagram of a prediction maximal-ratio diversity receiver. The signals are weighted proportionally to their individual rms signal envelope-to-mean noise power, and then summed. A predetection combiner requires a phase-control unit to cophase the individual signals. A number of cophasing and weighting techniques has been described in the literature [8],[18], [28],[29].

The CNR $\gamma$ of the resultant signal is

$$\gamma = \sum_{i=1}^{M} \gamma_i$$

and this is in contrast to selection diversity whose CNR is only the largest term $\gamma_i$. It is clear that in a maximal-ratio diversity system, an acceptable CNR can be obtained, even though none of the received signals is acceptable. Although it has the above-mentioned advantage over selection diversity, the maximal-ratio combiner involves complicated circuits for weighting, cophasing and summing the received signals.

From the CNR relation given above, the mean CNR $\overline{\gamma}$ of the resultant signal is obtained

$$\overline{\gamma} = M\gamma_o$$

This confirms the superiority of the maximal-ratio diversity technique.

The density function of $\gamma$ is given by [27]

$$p_M(\gamma) = \frac{\gamma^M}{\gamma_o^M (M-1)!} \exp\left(-\frac{\gamma}{\gamma_o}\right)$$

and the distribution function

$$\text{Prob}[\gamma_M \leq \gamma] = \int_o^\gamma p_M(\gamma)\, d\gamma$$

$$= 1 - \sum_{i=1}^{M} \frac{1}{(i-1)!} \left(\frac{\gamma}{\gamma_o}\right)^{i-1} \exp\left(-\frac{\gamma}{\gamma_o}\right)$$

The distribution function is plotted in Fig. 11. In comparison with selection diversity, at 99% reliability level, 2-branch maximal-ratio gives 11.5 db gain, and 4-branch gives 19 db gain, improvements of 1.5 db and 3 db, respectively.

*(d) Equal-Gain Diversity*

Tha maximal-ratio combiner requires some complicated circuit to achieve the correct weighting factors. The receiver can be made simpler by setting all the channel gains to unity, i.e. $g_i = 1$ in Fig. 10.

The distribution function of $\gamma$ can not be expressed in a closed form. It has been determined by numerical integration [12]. At all the reliability levels, the power savings, offered by equal-gain combiner, is only 1 db less than those of maximal-ratio, and therefore it is still better than selection diversity. It can still

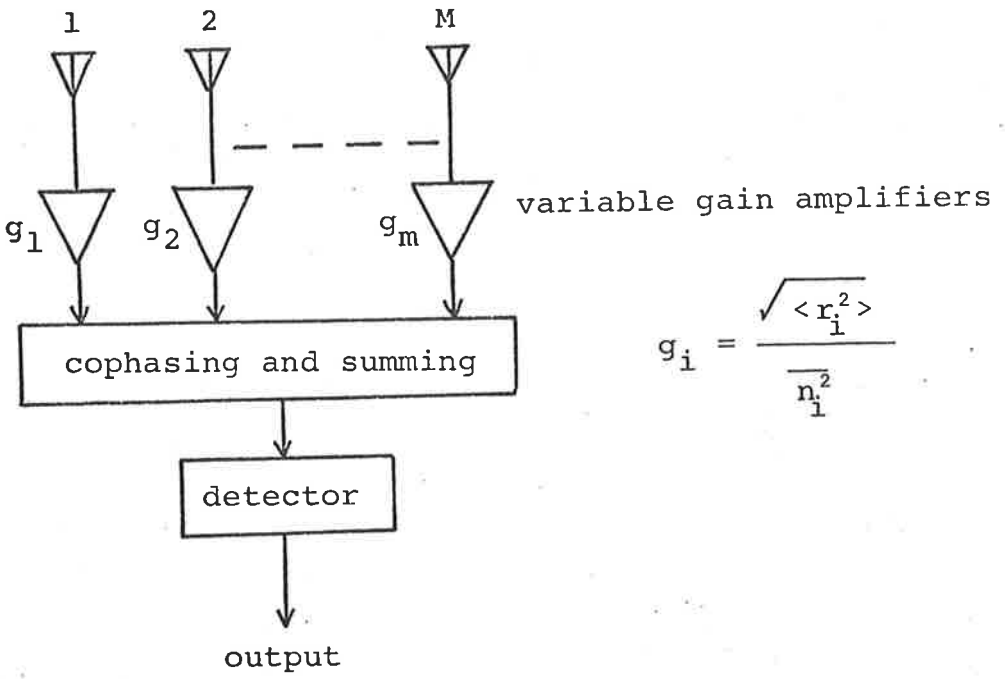


Fig. 10: Principle of a predetection maximal-ratio diversity receiver.

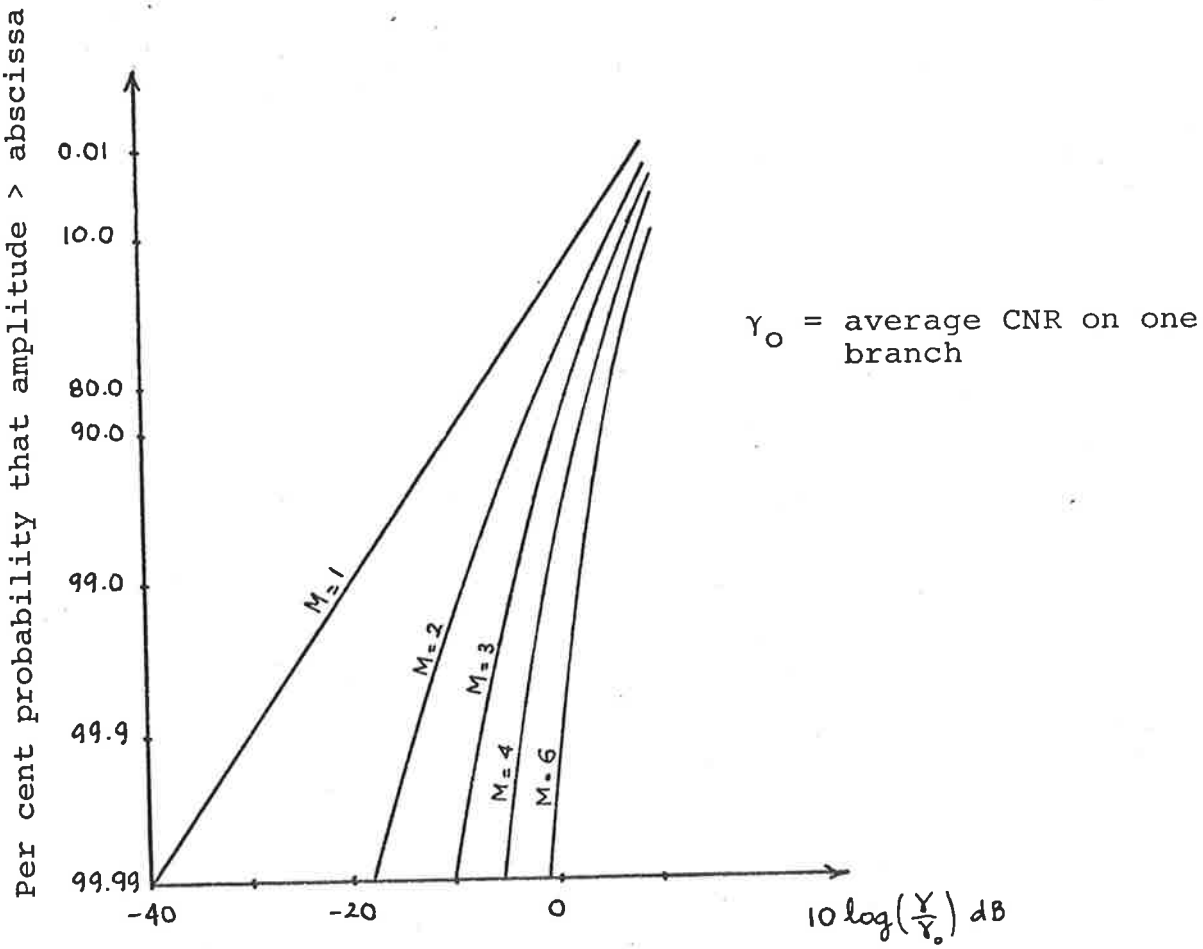


Fig. 11. Probability distribution of CNR $\gamma$ for M-branch maximal-ratio diversity system.

provide an acceptable resultant signal from a number of unacceptable individual signals.

The mean CNR $\overline{\gamma}$ of the resultant signal is [12]

$$\overline{\gamma} = [1 + (M-1)\frac{\pi}{4}]\gamma_o$$

It increases linearly with M as in the case of maximal-ratio diversity, but at a smaller rate.

*III.2 Pre- and Post-Detection Combining*

In systems where linear demodulation is used, in principle, it is irrelevant whether the combining is done before or after detection. However, in a predetection maximal-ratio or equal-gain combiner, the individual signals are required to be cophased.

In FM systems, where the threshold effect is pronounced [27], the results presented in Section A can not be applied for postdetection maximal-ratio and equal-gain combiners. An ideal two-branch postdetection maximal-ratio combiner has only 0.5 db advantage over selection combiner, compared with 2 db in the predetection case [27].

The full advantages of maximal-ratio and equal-gain diversity combining can only be realized in FM systems when predetection combining is used.

*III.3 Discussions*

It has been shown that with equal locally-incoherent noise inputs on diversity branches, maximal-ratio is marginally superior to equal-gain, and both methods are better than selection diversity. However, for two-branch diversity, the differences in power savings between the three techniques are quite small.

In Mobile Radio environment, the noise input to the diversity branches may be highly correlated due to noise sources in the vicinity of the mobile unit, such as the ignition systems of vehicles. It impairs the performance of maximal-ratio and equal-gain combiners, and in this case, selection diversity system becomes the better solution to the fading problem [12]. However, in a true selection diversity system, one receiver is required for each diversity branch, and the receiver outputs are required to be monitored continuously to select the best one at any instant. So a modified selection diversity receiver, known as switch diversity, is implemented. It offers a useful, attractive and economical alternative to the three well-known diversity techniques when the condition that the noise inputs are not locally incoherent, is not satisfied.

CHAPTER IV

# SWITCH DIVERSITY FSK SYSTEM IN MOBILE RADIO

## *IV.1 Introduction*

### *(a) Switch Diversity*

In a two-branch switch diversity receiver, one of two antennas is connected to the receiver by a switch. The envelope of the signal from the presently-connected antenna is monitored. If the signal envelope falls below some predetermined threshold, which can be either fixed, or variable, the switch is activated, and the other antenna is connected.

There are two switching strategies which can be used. They are switch-and-examine and switch-and-stay strategies. Switching from one antenna to the other occurs whenever a fade is detected. With the switch-and-examine strategy, if the signal on the second branch is above the predetermined threshold, switching stops. However if the signal switched to is also below threshold, the receiver input is switched back to the first antenna. It is switched rapidly between two antennas until it finds one above the threshold. With the switch-and-stay strategy, the receiver input stays with the second antenna whether it is acceptable or not.

Fig. 12 shows the different input signals to the receiver for the two strategies. It also shows the resultant signal if selection diversity is used. The selection diversity signal goes into deep fades only when both diversity signals fade simultaneously. The use of switch-and-stay strategy can cause the receiver to be switched to a branch entering deep fade, for example, at $t_1$ in Fig. 12. Switch-and-examine strategy can bring the receiver input signal back to an acceptable level more quickly, as shown in Fig. 12, following $t_1$ and $t_2$.

In predetection switch diversity receiver, switching results in switching transient noise due to the phase difference between branches. The transient noise will appear at the output of an FM discriminator as pulses whose width is proportional to the reciprocal of the IF bandwidth, and therefore the receiver performance will be degraded.

Although, the switch-and-examine strategy allows a quicker return to an acceptable level, rapid switching results in noise burst at the FM receiver output.

*(b) Binary Frequency-Shift-Keying (FSK)*

A binary FSK signal consists of constant-amplitude RF waveform having the instantaneous frequency shifted between two frequencies, one representing transmission of Mark, and the other, Space. It is received through

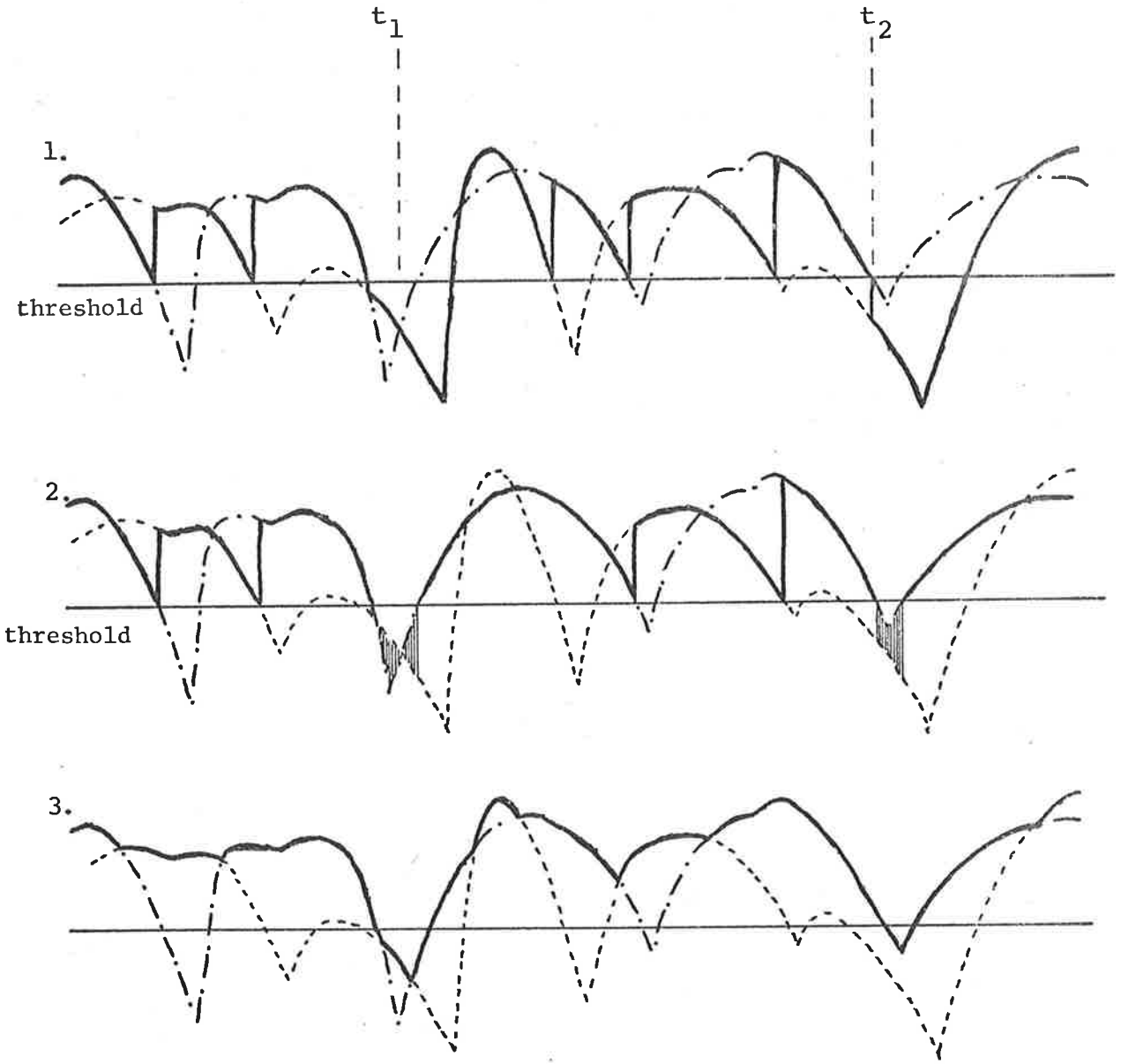


Fig. 12: Signal envelopes for

1. Switch-and-stay diversity
2. Switch-and-examine diversity
3. Selection diversity

$r_1$ represented by —·—·—·—
$r_2$ represented by ----------
$r_3$ represented by ——————
$r_1$ and $r_2$ are the received signal envelope
R is the resultant signal envelope.

a pair of band-pass filters (BPF), see Fig. 13, in a non-coherent FSK demodulator. The BPF's have one centered on the Mark frequency, and one on the Space frequency. The FSK detector output is decided by comparing the envelopes of the filter outputs. The actual binary decision is made by sampling the detector output. Errors arise because of additive Gaussian noise and interference.

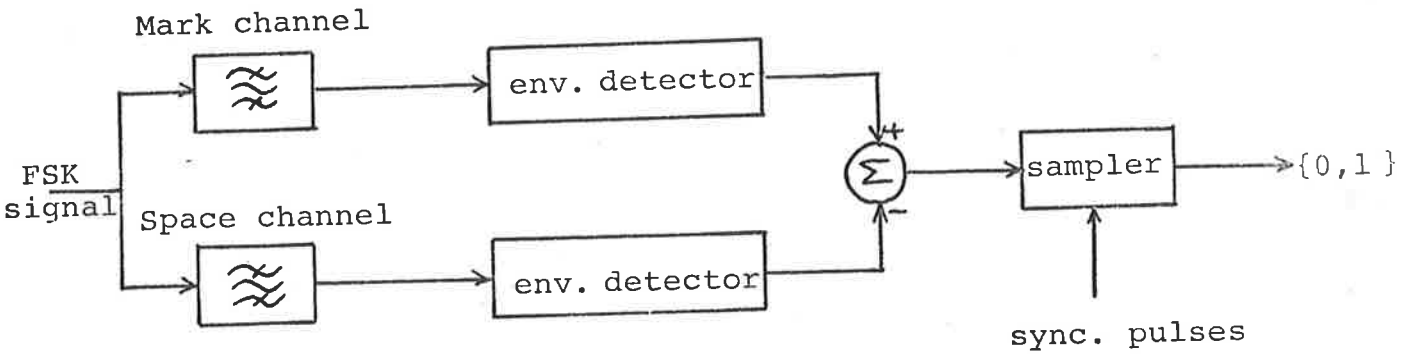


Fig. 13: Principle of a non-coherent FSK demodulator.

In an On-Off Keying receiver (OOK), the optimum detection threshold is a function of signal amplitude, and therefore it must be continually adjusted in Mobile Radio environment [16]. While the FSK optimum detection threshold is a zero level, and is independent of the signal amplitude. Thus, an FSK detector inherently contains the performance of a continuously optimized variable threshold system. For this reason, FSK is preferred to OOK in a fading environment.

*IV. 2 Theoretical Studies of Switch Diversity*

A two-branch switch diversity using switch-and-stay strategy is considered.

Assuming that the signal envelopes $r_1$ and $r_2$, received at the mobile antennas, follow Rayleigh distribution [3]-[7] and are independent of each other. Their means and autocorrelations are also assumed to be the same. Their density functions are given by

$$p(r) = \begin{cases} \frac{r}{b_o} \exp\left(-\frac{r^2}{2b_o}\right) & r \geq 0 \\ 0 & r < 0 \end{cases}$$

$$r^2_{rms} = 2b_o$$

and their cumulative distribution functions are

$$P_r(A) = \text{Prob}[r \leq A]$$

$$= 1 - \exp\left(-\frac{A^2}{2b_o}\right)$$

Let T be the switching threshold. The resultant signal R(t) consists of segments X and Y from $r_1(t)$ and $r_2(t)$. The typical segments X and Y are shown in Fig. 14. The starting point $R_o$ of each segment can be either below or above T.

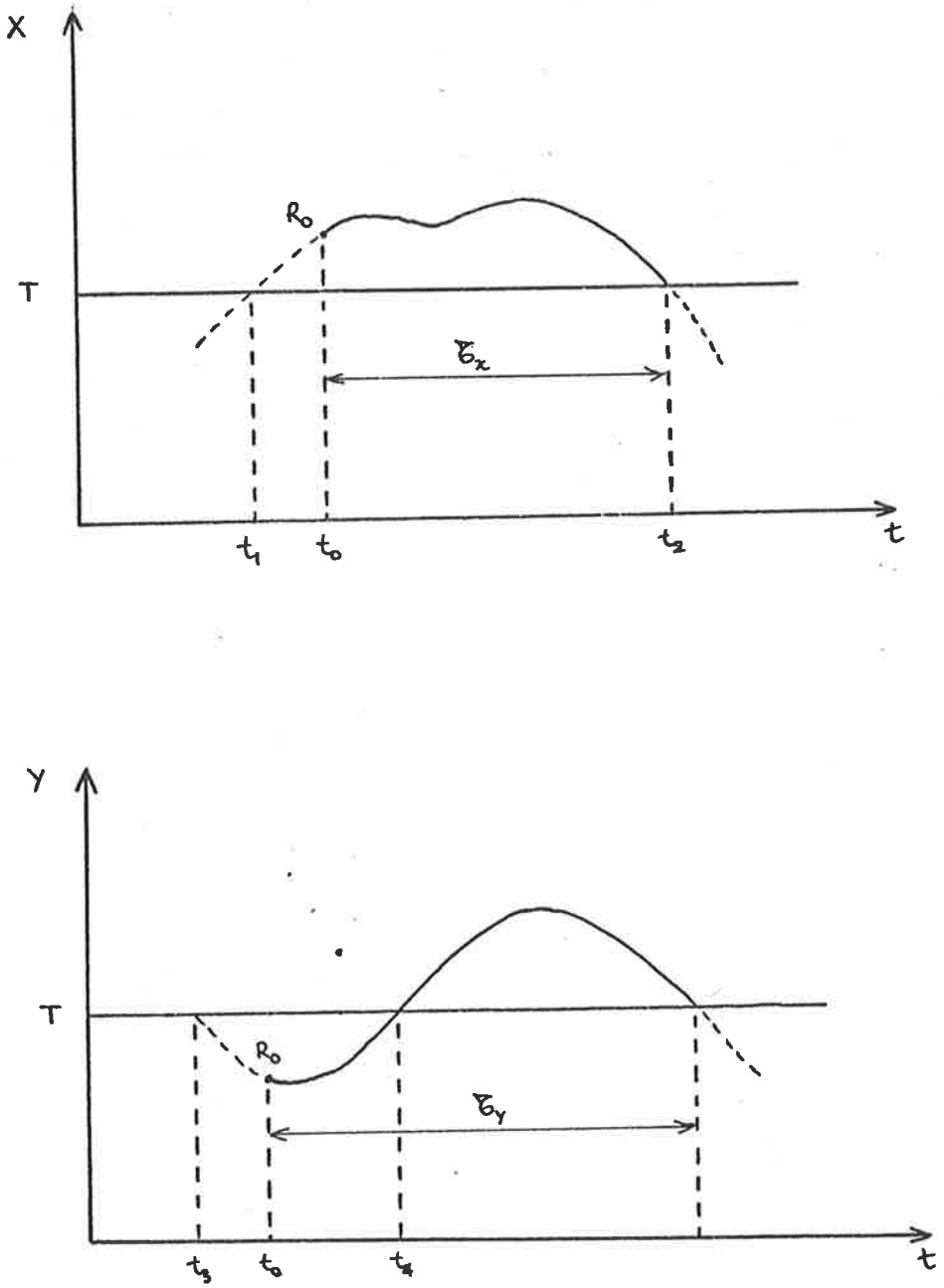


Fig. 14: Typical segments X and Y of the resultant signal envelope R.

Assuming that segments of $r_1$ and $r_2$ are independent of each other [13], the probability of $R_o$ to be above T is given by

$$p = \text{Prob}[R_o > T] = 1 - \text{Prob}[R_o \leqslant T]$$

$$p = \exp\left(-\frac{T^2}{2b_o}\right)$$

p is called the probability of a successful switching. The probability of an unsuccessful switching is

$$q = \text{Prob}[R_o \leqslant T] = 1 - \exp\left(-\frac{T^2}{2b_o}\right)$$

Since $r_1$ and $r_2$ are indistinguishable, see Fig. 13,

$$\begin{aligned} P[R \leqslant A] &= P[R \leqslant A/R = r_1] \\ &= P[R \leqslant A/R = r_2] \\ &= P[r \leqslant A] = P_r(A) \\ &= 1 - \exp\left(-\frac{A^2}{2b_o}\right) \end{aligned}$$

The average duration when R(t) is above T is

$$\tau_p = \frac{p}{q}\,\tau_q$$

where $\tau_q$ represents the average duration when R(t) fades below T.

The starting point $R_o$ of segments X can be anywhere between $t_1$ and $t_2$, so the average duration $\tau_x$ of X is given by

$$\tau_x = \frac{\tau_p}{2}$$

and the starting point $R_o$ of segments Y can be anywhere between $t_3$ and $t_4$; this gives the average duration $\tau_y$ of Y

$$\tau_y = \tau_p + \frac{\tau_q}{2}$$

The conditional probability that $R \leqslant A$ when the signal in use is above T, can be written as

$$P[R \leqslant A/r > T] = \frac{P[r \leqslant A, r > T]}{P[r > T]}$$

$$= \begin{cases} \dfrac{P_r(A) - q}{1-q} & A \geqslant T \\ 0 & A \leqslant T \end{cases}$$

and the conditional probability that $R \leqslant A$ when the signal in use is below T, is

$$P[R \leqslant A/r \leqslant T] = \frac{P[r \leqslant A, r \leqslant T]}{P[r \leqslant T]}$$

$$= \begin{cases} 1 & A \geqslant T \\ \dfrac{P_r(A)}{q} & A \leqslant T \end{cases}$$

Combining the above conditional probability functions, the distribution function of the resultant signal envelope R is obtained

$$P[R \leqslant A] = P[R \leqslant A/r > T] \frac{p\frac{\tau_p}{2} + q\tau_q}{p\frac{\tau_p}{2} + q\tau_q + q\frac{\tau_q}{2}}$$

$$+ P[R \leqslant A/r \leqslant T] \frac{q\frac{\tau_q}{2}}{p\frac{\tau_p}{2} + q\tau_q + q\frac{\tau_q}{2}}$$

After some manipulation it can be shown that

$$P[R \leqslant A] = \begin{cases} (1 + q)\, P_r(A) - q & A \geqslant T \\ q\, P_r(A) & A \leqslant T \end{cases}$$

Differentiating the distribution function, the density function of R is obtained

$$p_r(A) = \begin{cases} (1 + q)\, p_r(A) & A > T \\ q\, p_r(A) & A < T \end{cases}$$

The distribution curves are plotted in Fig. 15 for various fixed threshold levels relative to $r_{rms}$. For comparison, the Rayleigh and ideal two-branch selection diversity distribution curves are also shown.

At the switching threshold

$$P[R \leqslant T] = q^2 = P[R \leqslant T/\text{selection diversity}]$$

The switch diversity curves touch the selection diversity curve at the threshold. Below the threshold, the curves have Rayleigh slope but are displaced by an amount equal to the threshold. Above the threshold, they merge with the Rayleigh curve, but this should not cause any concern since diversity has most to offer at low signal levels only.

Since the switch control circuit can not have an infinite bandwidth, so there is always a switching time delay between the threshold crossing and switching. The distribution of R will be degraded because the signal continues to go into deep fade below threshold before switching occurs.

For the switching time delay $\tau_D$ is small, compared with $\tau_q$, the average duration of fades below T, Rustako [13] derived the distribution of R

$$P[R < A] = \begin{cases} \dfrac{\tau_q}{\tau_q + 2q\tau_D}\,[q\,P_r(A) + P_r(A) - q] + \dfrac{2q\tau_D}{\tau_q + 2q\tau_D} & A \geqslant T \\ \dfrac{\tau_q}{\tau_q + 2q\tau_D}\,q\,P_r(A) + \dfrac{2q\tau_D}{\tau_q + 2q\tau_D}\left[1 - \operatorname{erf}\left(\dfrac{A - T}{\omega_m \tau_D \sqrt{b_o}}\right)\right. & \\ \qquad \left. + \dfrac{A - T}{\sqrt{\pi b_o}\,\omega_m \tau_D}\, E\left(-\dfrac{(A - T)^2}{\omega_m^2 \tau_D^2 b_o}\right)\right] & A \leqslant T \end{cases}$$

$$\text{where } \operatorname{erf}(x) = \frac{2}{\sqrt{\pi}} \int_0^x e^{-t^2} dt$$

$$E(x) = \int_{-\infty}^{x} \frac{e^t}{t} dt$$

$$\omega_m = 2\pi f_m$$

The distribution curve of R is presented in Fig. 16 for $\tau_D/\tau_q = 0.144$. It shows that for $\tau_D/\tau_q \leq 0.144$, the degradation due to the switching time delay is negligible.

Let $\tau_{Dmax}$ be the maximum tolerable switching time delay

$$\tau_{Dmax} = 0.144\ \tau_q$$

it is presented in Fig. 17 as a function of the threshold T for $f_c = 500$ MHz and v = 90 km/hr.

### *IV.3 Error Rates of a Non-Coherent FSK Receiver Using Switch Diversity*

In the presence of Gaussian white noise, a non-coherent FSK receiver gives the error probability, conditional on the CNR [27]

$$P[\text{error}/\gamma] = \frac{1}{2} \exp\left(-\frac{\gamma}{2}\right)$$

$$\text{where CNR } \gamma = \frac{r^2}{2N}$$

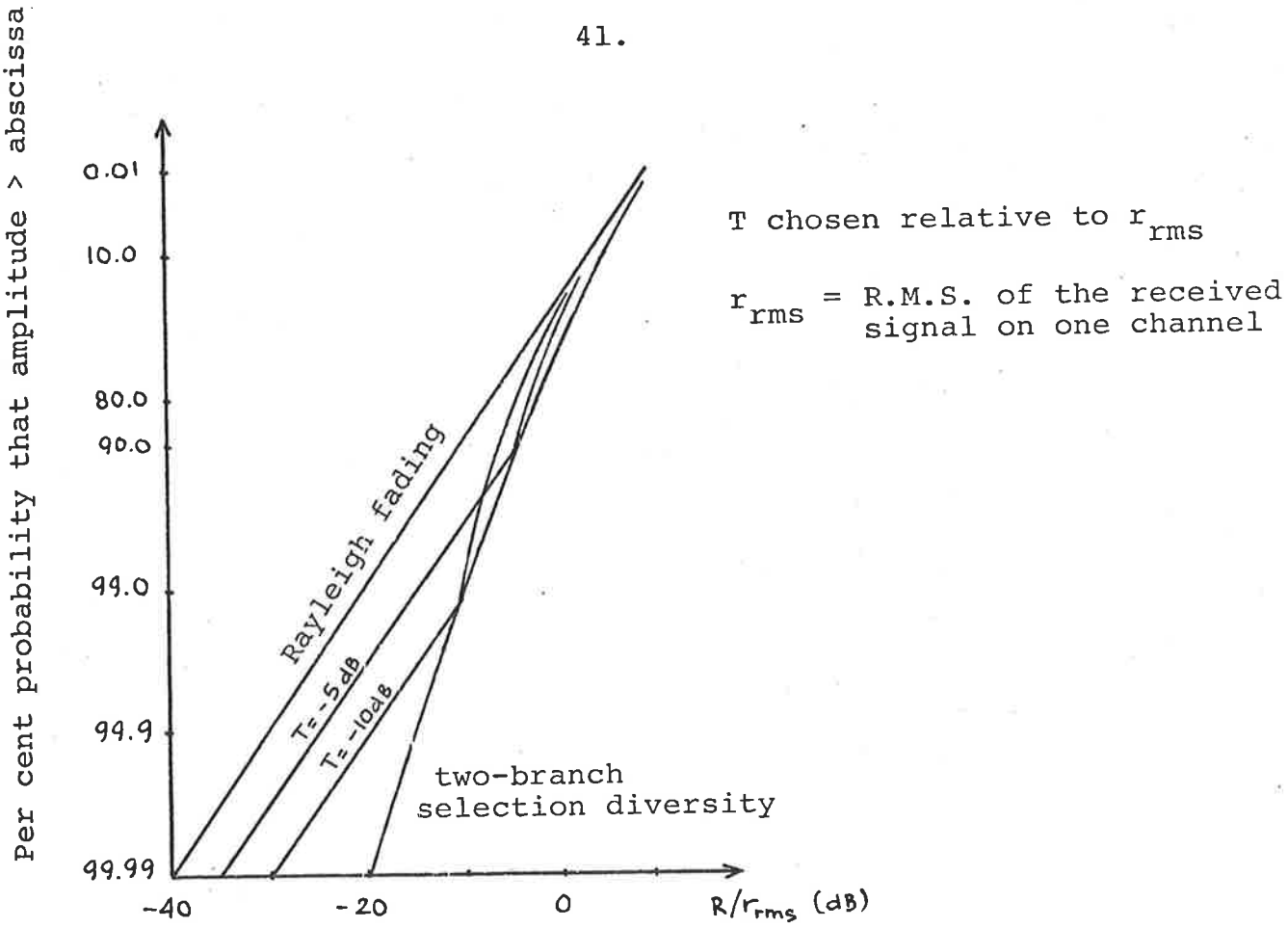


Fig. 15: Probability distribution for two-branch switch diversity using switch-and-stay strategy.

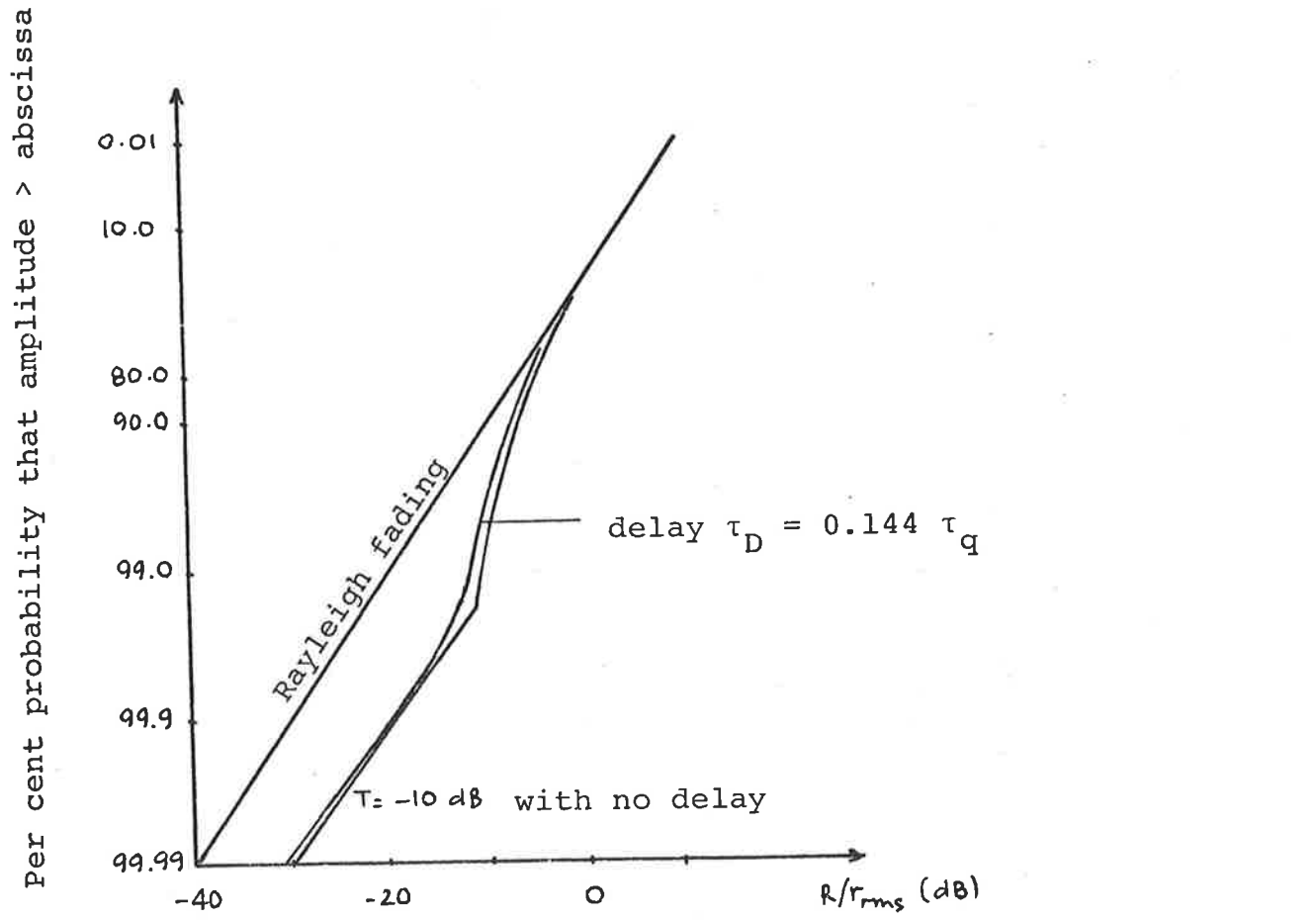


Fig. 16: Probability distribution for two-branch switch diversity using switch-and-stay strategy with switching delay.

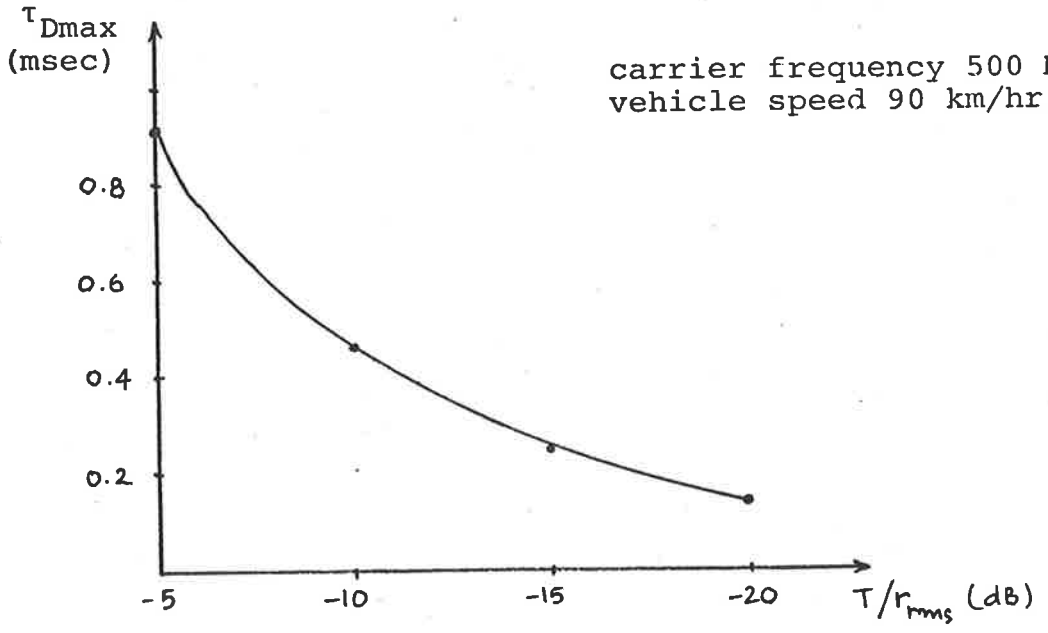


Fig. 17: Maximum tolerable switching time delay.

$\frac{r^2}{2}$ = total signal power

N = predetection noise power per branch.

In the Rayleigh fading environment, the CNR $\gamma$ has the density function

$$p(\gamma) = \frac{1}{\gamma_o} \exp\left(-\frac{\gamma}{\gamma_o}\right) \qquad \gamma_o = \langle\gamma\rangle$$

Therefore, the average error probability is

$$\bar{P}_e = \int_0^\infty P[\text{error}/\gamma]\, p(\gamma)\, d\gamma$$

$$= \frac{1}{2 + \gamma_o}$$

Using the density function of the CNR $\gamma$ for a two-branch selection diversity

$$p(\gamma) = \frac{2}{\gamma_o} \left[1 - \exp\left(-\frac{\gamma}{\gamma_o}\right)\right] \exp\left(-\frac{\gamma}{\gamma_o}\right)$$

the average error probability for an FSK using two-branch selection diversity can be derived

$$\bar{P}_e = \frac{1}{2 + \gamma_o} \times \frac{1}{1 + \frac{\gamma_o}{4}}$$

These average error rates are plotted in Fig. 18.

From the density function of the switch diversity resultant signal R given in Section IV.2, it follows that

$$p(\gamma) = \begin{cases} \frac{1}{\gamma_o}\left[2 - \exp\left(-\frac{T^2}{2b_o}\right)\right] \exp\left(-\frac{\gamma}{\gamma_o}\right) & A > T \\ \frac{1}{\gamma_o}\left[1 - \exp\left(-\frac{T^2}{2b_o}\right)\right] \exp\left(-\frac{\gamma}{\gamma_o}\right) & A < T \end{cases}$$

And the average error probability can be obtained

$$\bar{P}_e = \frac{1}{2 + \gamma_o}\left[2 - \exp\left(-\frac{T^2}{2b_o}\right)\right] \exp\left(-\frac{2 + \gamma_o}{2} \cdot \frac{T^2}{2b_o}\right)$$

$$+ \frac{1}{2 + \gamma_o}\left[1 - \exp\left(-\frac{T^2}{2b_o}\right)\right]\left[1 - \exp\left(-\frac{2+\gamma_o}{2} \cdot \frac{T^2}{2b_o}\right)\right]$$

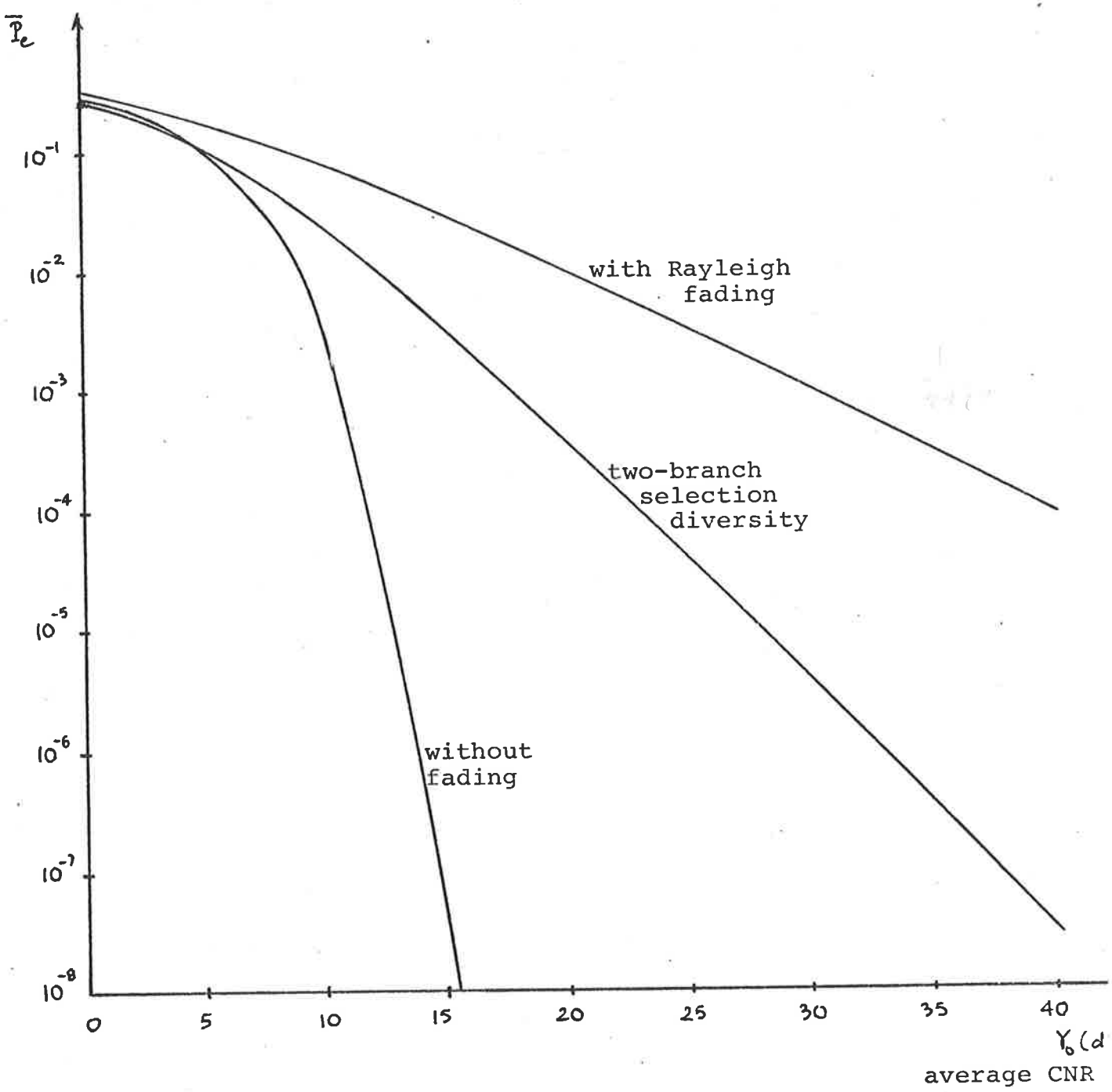


Fig. 18: Error rates for ideal non-coherent FSK receiver.

Fig. 19 shows the average error rates for various fixed threshold levels relative to $r_{rms}(= 2b_o)$.

Let the derivative to $\overline{P}_e$ relative to $\frac{T^2}{2b_o}$ equal to zero the optimum threshold is found

$$\frac{T^2_{opt}}{2b_o} = \frac{2}{\gamma_o} \ln (1 + \frac{\gamma_o}{2})$$

and presented in Fig. 20. The average error rate for the optimum threshold is shown in Fig. 21.

The mean value of the resultant signal envelope R

$$<R> = q \int_o^T r\, p(r)\, dr + (1 + q) \int_T^\infty r\, p(r)\, dr$$

$$= (1 + q) \sqrt{\frac{\pi}{4}}\, r_{rms} + T \exp (- \frac{T^2}{r^2_{rms}})$$

$$- \frac{\sqrt{\pi}}{2}\, r_{rms}\, \text{erf} (\frac{T}{r_{rms}})$$

where the error function

$$\text{erf} (\frac{T}{r_{rms}}) = \frac{2}{\sqrt{\pi}} \int_o^{\frac{T}{r_{rms}}} \exp (- x^2)\, dx$$

$$\frac{<R>}{T} = [(1 + q) \sqrt{\frac{\pi}{4}} - \frac{\sqrt{\pi}}{2} \text{erf} (\frac{T}{r_{rms}})] \frac{r_{rms}}{T}$$

$$+ \exp (- \frac{T^2}{r^2_{rms}})$$

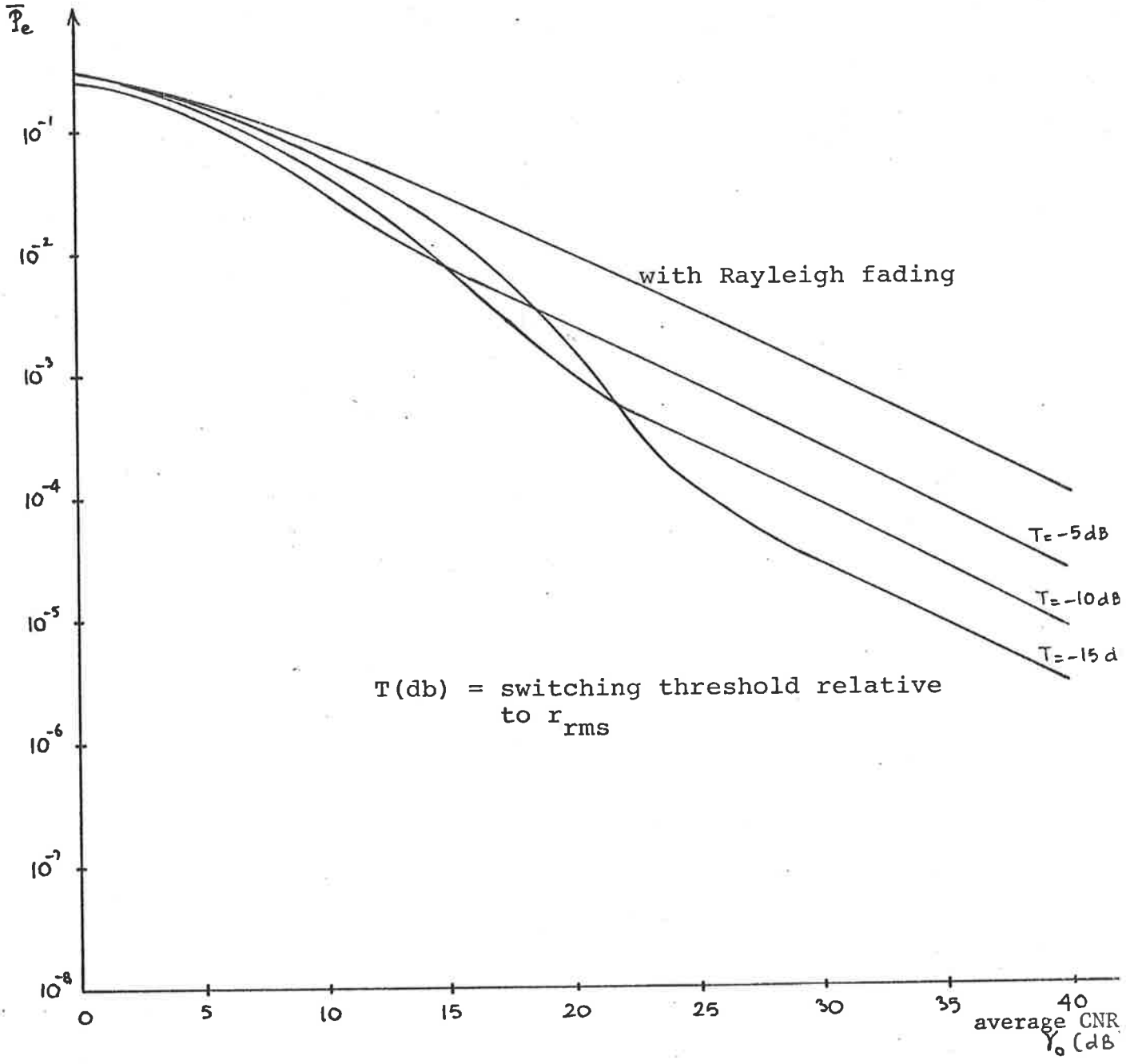


Fig. 19: Error rates for ideal non-coherent FSK receiver.

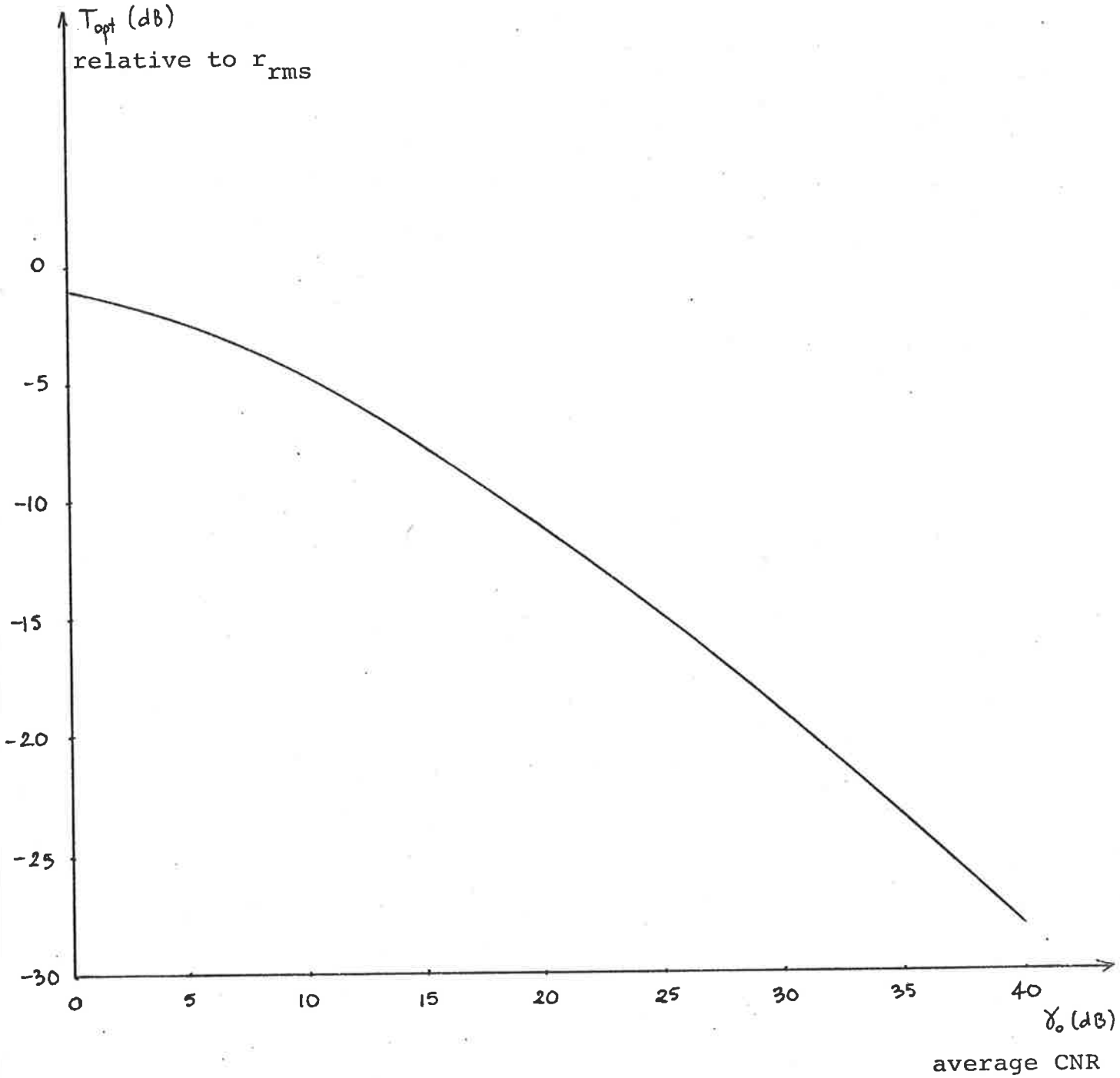


Fig. 20: Optimum switching threshold level for non-coherent FSK.

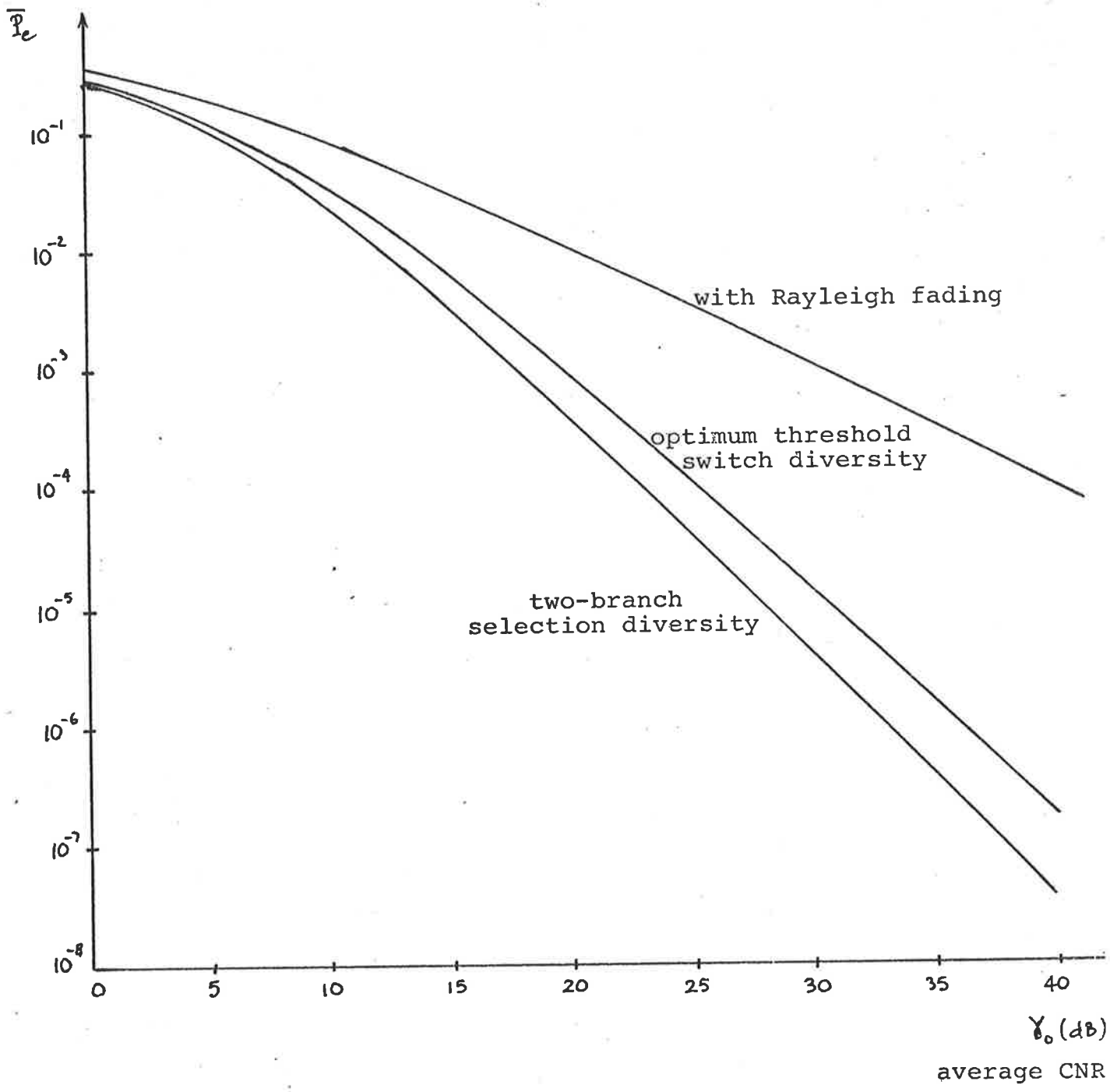


Fig. 21: Error rates for ideal non-coherent FSK receiver.

Therefore, for every fixed threshold relative to $r_{rms}$, there is a corresponding fixed threshold relative to $<R>$. And the relation between $\frac{T}{r_{rms}}$ and $\frac{T}{<R>}$ can be obtained from the above expression.

*IV. 4 Some Practical Aspects of Switch Diversity*

The fading information of the received signal can be obtained by measuring the signal envelope. However, in practice, it is the envelope of signal-plus-noise that is measured.

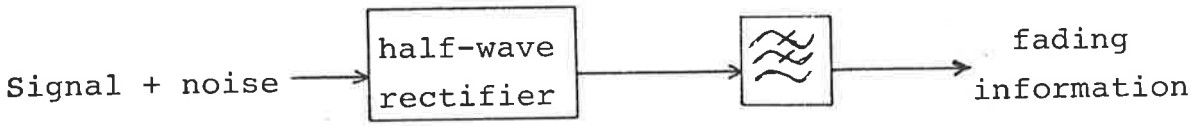


If a simple diode is used as a half wave rectifier, the measured envelope will be less than the actual envelope by an amount equal to the diode forward voltage. The cut-off frequency of the low-pass filter (LPF) must be low to remove any high frequency noise not related to fading. However, it must not be too low to introduce intolerable switching time delay. At 1000 MHz and 90 km/hr, the maximum tolerable switching time delay is 0.2 msec, at the threshold level -10 db relative to $r_{rms}$, therefore the cut-off frequency of the LPF should be at least 5 KHz.

The LPF output is fed through a high-pass filter (HPF) to remove the mean value of the resultant signal envelope, the fading information is allowed to pass.

The cut-off frequency of the HPF must be high enough to block the slow fading of the input signal which occurs when the mobile unit moves from one area to another. Therefore, its cut-off frequency depends on the vehicle speed and the effect of environment. The HPF output, which is the resultant signal envelope with zero mean is then compared with a negative voltage in the comparator. The threshold setting can be fixed or variable below the mean signal input. A switch command is generated whenever the HPF output falls below the switching threshold.

The input signal-plus-noise could give a false information on fading. Hysteresis in comparator can be used to eliminate false switchings. The amount of hysteresis depends on the noise power, and also on the signal power. After switching occurs, if the second input is above threshold but within the hysteresis region, it will be interpreted as a fade, i.e. below threshold. When it falls below threshold, no switching will take place. Therefore the amount of hysteresis should be greater than the mean noise envelope and much smaller than the mean signal envelope to reduce the number of false switchings and also "miss" switchings.

CHAPTER V

# EXPERIMENTAL SWITCH DIVERSITY FSK RECEIVER

A two-branch switch diversity FSK receiver using switch-and-stay strategy and non-coherent FSK demodulator has been designed and constructed in the laboratory. The receiver was tested using two simulated independently Rayleigh fading signals generated by the fading simulator, constructed by Davis [30]. The error rates of the receiver were obtained under various conditions and compared with the theoretical predictions. This simple experimental receiver is used only to back up the theoretical error rates obtained in Section IV.3. Many practical aspects, which introduce the non-ideality into the system and were discussed in Section IV.4, are quite complex and not investigated.

In this work, perfect time recovery and timing were assumed.

## *V.1 Implementation of the Receiver*

Fig. 22 shows the simplified block diagram of the experimental receiver. The receiver was designed to handle bit rates of up to 56 Kbits/sec, and was without the circuit to measure the zero-mean input signal level (see Section IV.4). A knowledge of the rms value of the received signal envelope $r_{rms}$ enables the switching threshold to be chosen relative to $r_{rms}$.

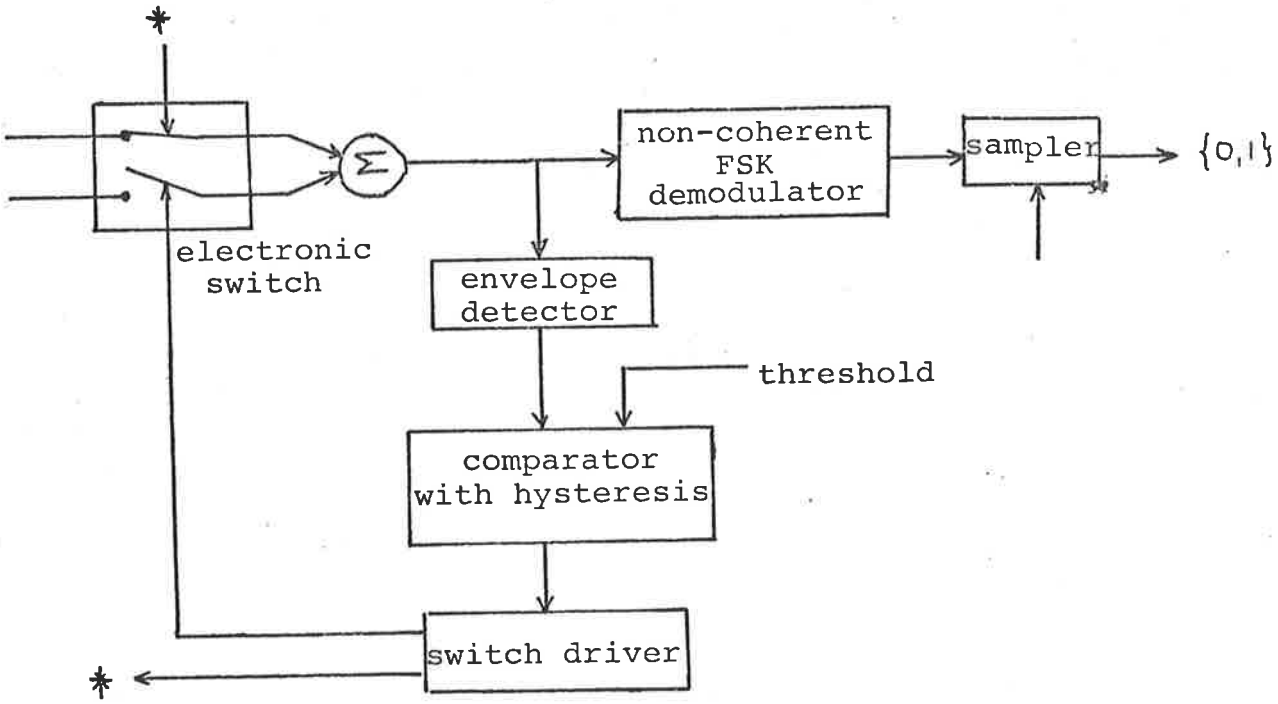


Fig. 22: Simplified block diagram of the experimental receiver.

*(a) Non-Coherent FSK Demodulator*

The demodulator is shown in Fig. 23.

The BPF's are two simple LC tuned circuits whose 3-db bandwidth is 56 KHz. To reduce the intersymbol interference and crosstalk, the Mark frequency is chosen to be at 1.1 MHz and the Space frequency 0.9 MHz. Their outputs are fed to two simple envelope detectors, each consisting of a diode followed by a LPF.

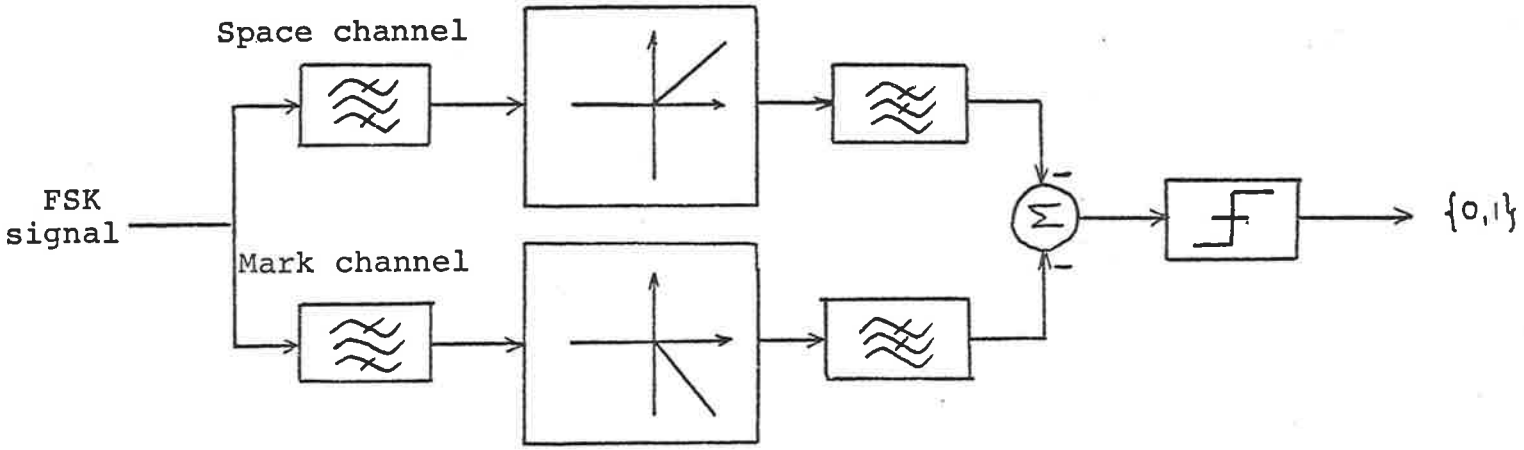


Fig. 23: Block diagram of the non-coherent FSK demodulator

In the Mark channel, the half-wave rectifier responds only to the negative half-cycles, and the half wave rectifier of the Space channel responds to the positive half cycles.

The LPF's are the 4th order Butterworth low-pass filters with the cut-off frequency of 2$\theta$ KHz. The channel outputs are inverted, summed, and fed through a zero-level comparator, and then sampled.

The detailed circuit of the demodulator is shown in Appendix A.

*(b) Fade Detector*

Fig. 24 shows the block diagram of the fade detector.

The input signal is envelope-detected by passing through a diode and a 4th order Butterworth LPF with the cut-off frequency of 9 KHz. The signal envelope is compared with a fixed direct voltage $V_T$ which is chosen to be some amount below the measured $r_{rms}$ of the input signal.

The comparator output drives the clock input of a J/K flip flop. The outputs Q and $\overline{Q}$ of the flip flop change level whenever the input signal envelope crosses the threshold in the negative direction.

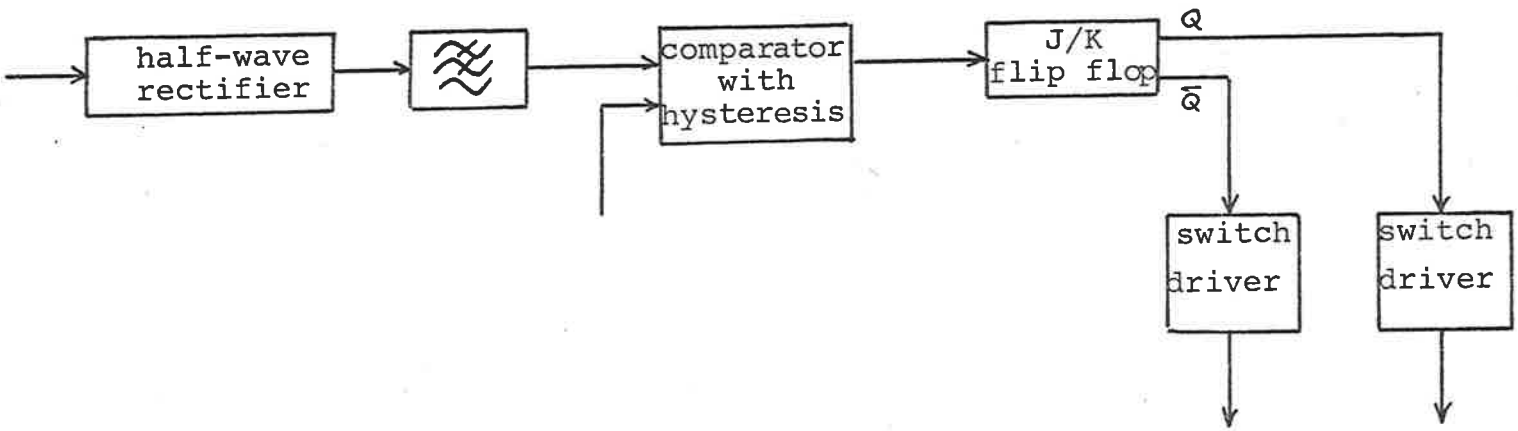


Fig. 24: Block diagram of the fade detector.

As discussed in Section IV.4, a comparator with inbuilt hysteresis is used to avoid false switchings. The switching actually occurs when the envelope detector output falls below $(V_T - 0.05)V$. To avoid "miss" switchings, the envelope has to be above $(V_T + 0.36)V$.

The detailed circuit of the fade detector is presented in Appendices B and C.

*V.2 Experimental Results*

The experimental setup is shown in Fig. 25. The pseudo-random number generator generates binary digit at a rate of 30 Kbits/sec, and the test was carried out at this bit rate.

Generating the delayed input data and synchronous pulses is described in Fig. 26.

The signal and noise power were measured on a true RMS voltmeter. With no noise input, the signal power was measured at the BPF input, and with no signal input, the noise power was measured at the BPF output. The ratio of two readings, corrected by the loss caused by the BPF, gave the CNR. The signal power reading enabled the switching threshold to be chosen, relative to $r_{rms}$.

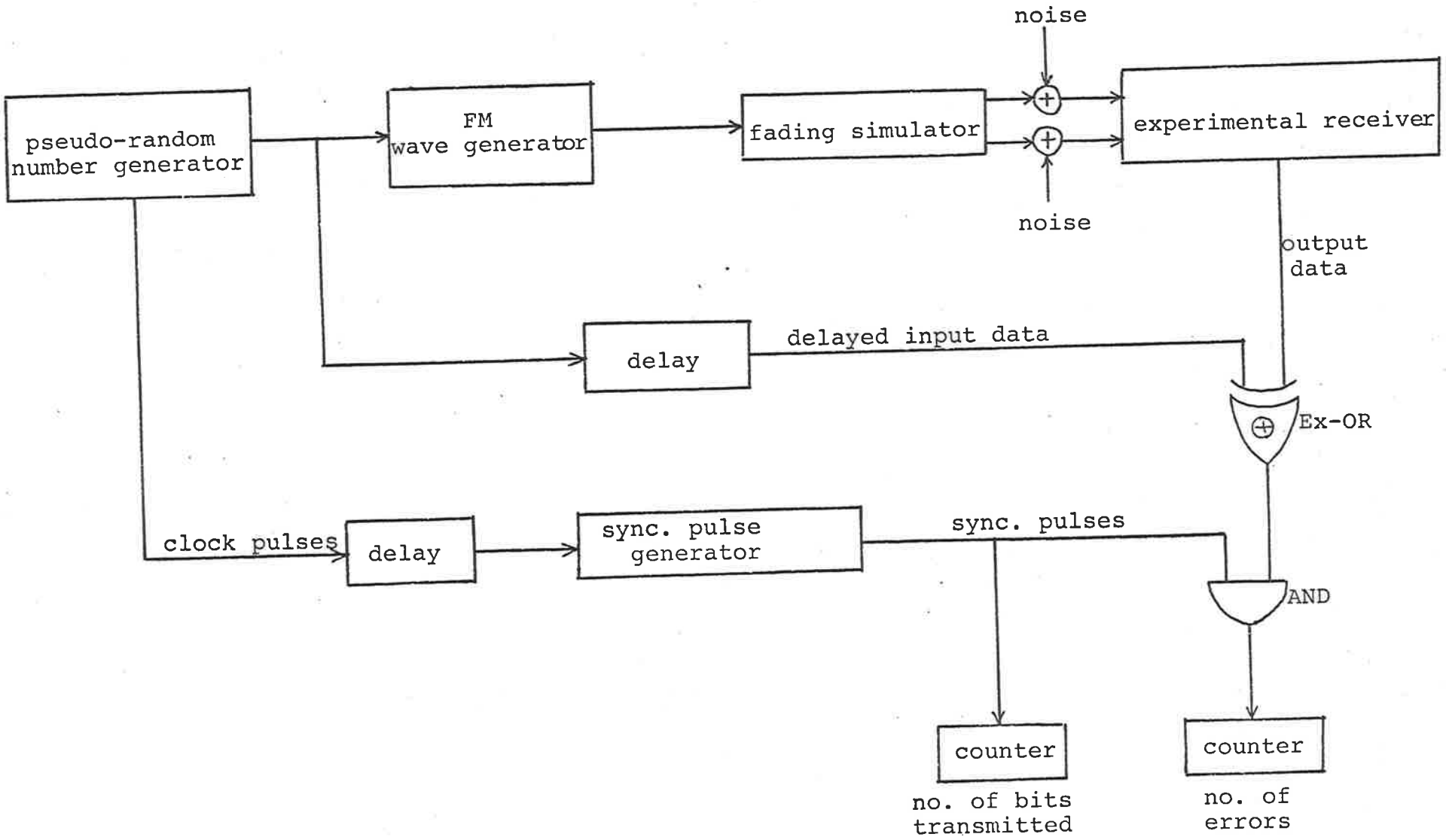


Fig. 25: Experimental set up.

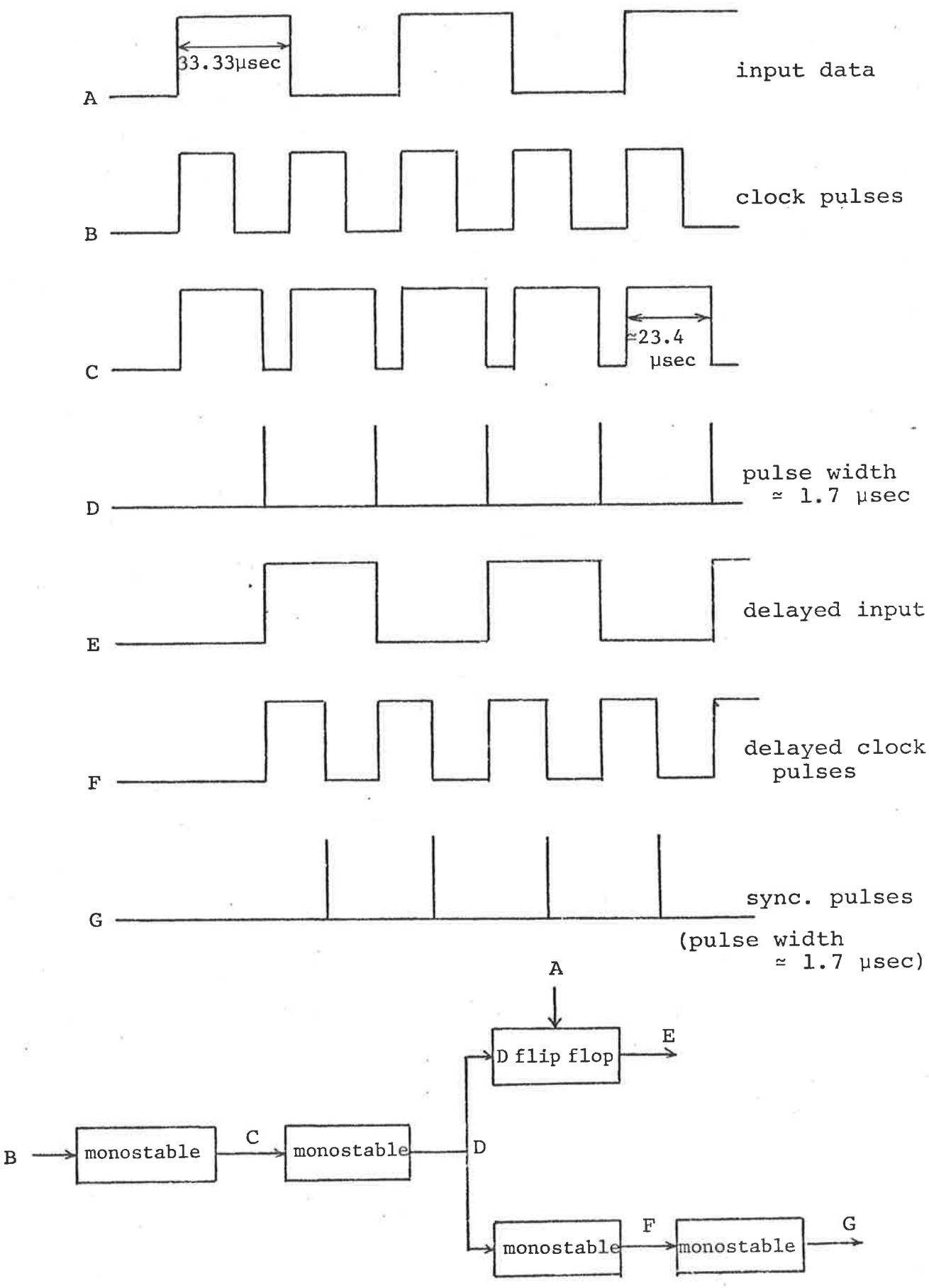


Fig. 26: Generating delayed input and synchronous pulses.

*(a) Non-Fading Case*

The output of the FM wave generator was amplified to produce a 6V peak-to-peak signal and then added to random noise. The error rates given as the ratio of the readings of two counters, were obtained for every half an hour for various CNR's. The experimental results are shown in Fig. 27 together with the ideal-case curve. At low signal levels, the receiver performance is about 2 db worse than that of an ideal receiver. The major contribution to the difference is the diode forward voltage in the half wave rectifiers. The difference decreases when the CNR increases. The factor contributing to this is that the error probability expression of an ideal non-coherent FSK receiver is applied correctly only when CNR is much greater than one [27], and when the signal level is increased, the effect of the diode forward voltage is reduced.

*(b) Fading Without Switch Diversity*

The $r_{rms}$ of the input signal was about 3V. The value was chosen to reduce the effect of the diode forward voltage and the number of "miss" switchings due to the hysteresis in the comparator when diversity was in use.

Fig. 28 shows the receiver performance. It agrees quite well with the theoretical prediction.

*(c) Fading With Switch Diversity*

The switching threshold was set at 10 db below $r_{rms}$. The error rates were obtained for two different fading

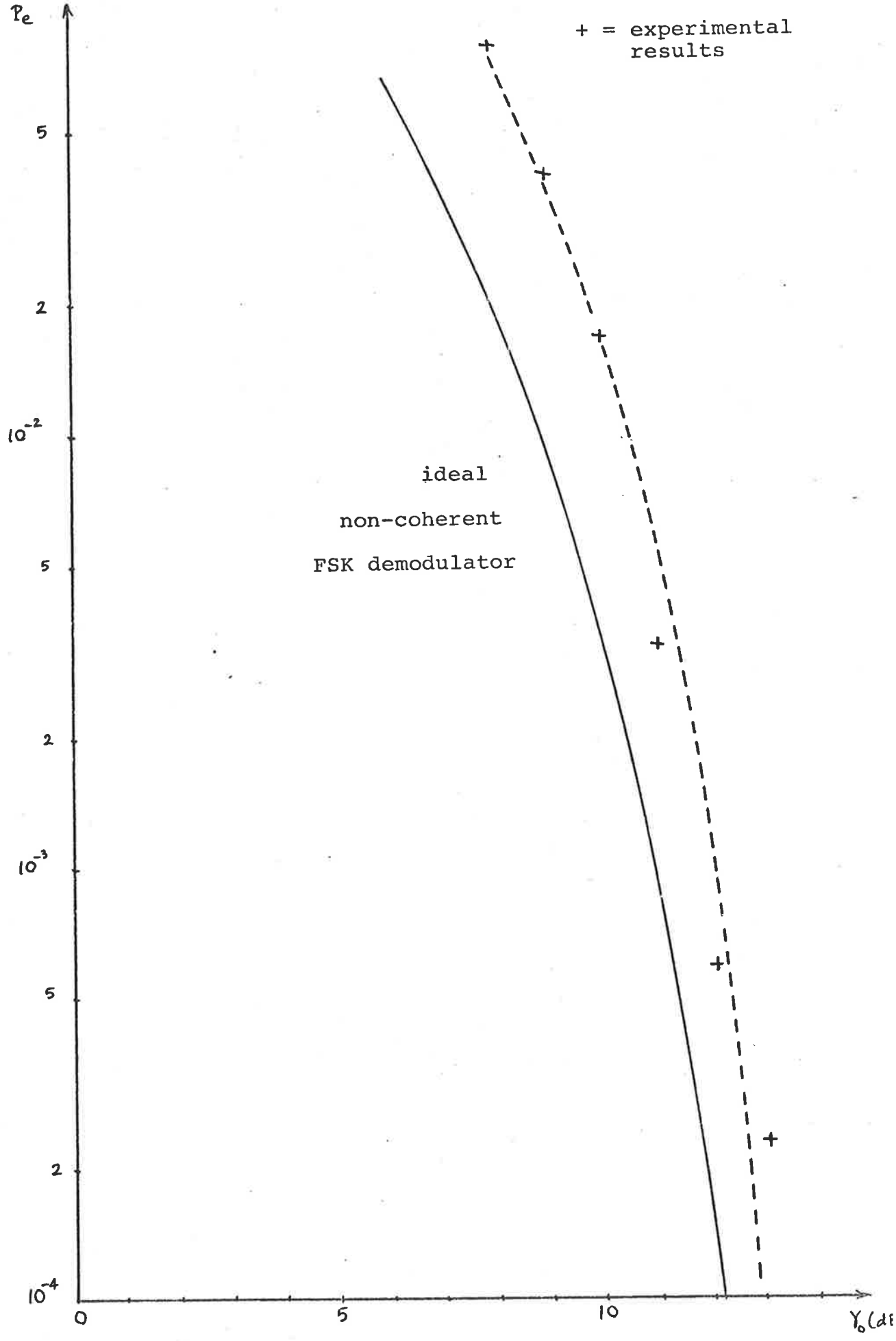


Fig. 27: Error probability in non-fading case.

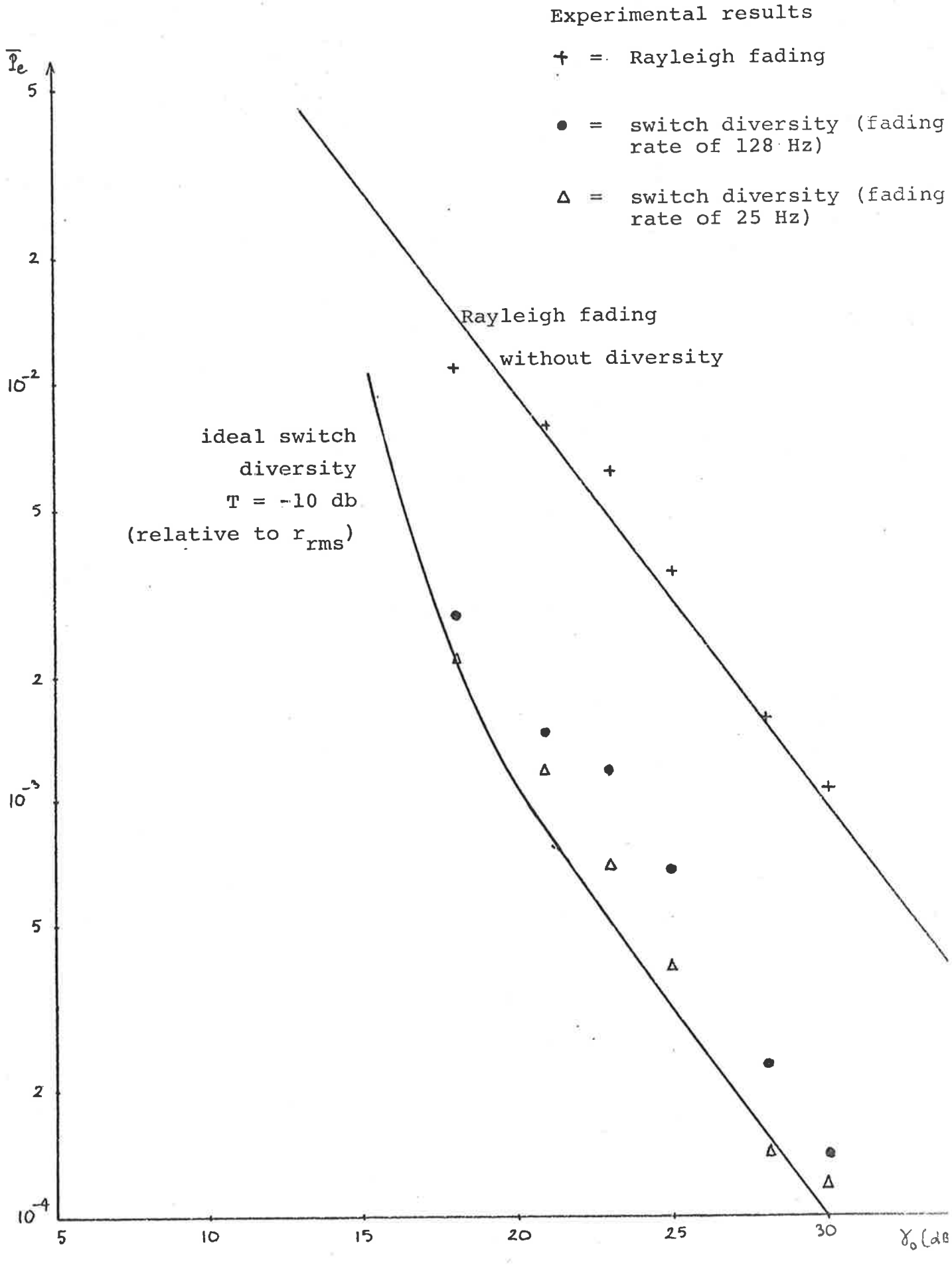


Fig. 28: Average error rates in Rayleigh fading environment, with and without switch diversity.

rates of 25 Hz and 128 Hz, where the fading rate is twice the maximum Doppler shift $f_m$. At the carrier frequency of 900 MHz, the first fading rate corresponds to a vehicle speed of 15 km/hr, and the second to a speed of 77 km/hr.

The experimental results agree reasonably well with the theoretical prediction. There is a number of factors contributing to the difference between the theoretical curves and the experimental one:

(i) the diode forward voltage,

(ii) the actual switching threshold was greater than -10 db, relative to rms, due to the operation used to detect the fading, see Section IV.4 (using envelope detector), and

(iii) the effect of hysteresis in the comparator.

For the difference between the results of two fading rates, a possible explanation may lie in the use of hysteresis and in obtaining the fading information. These problems are quite complex, and not investigated in this work.

CHAPTER VI

# CONCLUSION

It has been shown that in Mobile Radio, the error rates of data transmission using FSK is drastically deteriorated, and the use of switch diversity can recover some of the loss caused by fading. It has also been pointed out that switch diversity is an economical alternative to selection diversity.

The error rates were calculated for various switching threshold settings which were fixed relative to the rms received signal envelope $r_{rms}$, and in turn, they are fixed relative to the mean value of the resultant signal envelope. A possible implementation of the fixed threshold setting relative to the mean was outlined.

For the switching threshold of -10 db relative to the $r_{rms}$, the experimental results show a quite close agreement to the theoretical prediction. At reasonable error rates from $10^{-3}$ to $10^{-4}$, switch diversity offers an improvement of about 7 db. The difference between the experimental results and the theoretical ones, and also the difference between the experimental results for different fading rates are caused by the non-ideal envelope detectors, false switchings due to noise, and "miss" switchings due to the use of hysteresis in comparator. These problems are very complex, and were not investigated. The performance degradation of the receiver due to vehicle ignition noise

was also not studied.

In switch-and-stay diversity, it would be profitable to prevent the receiver from being connected to a signal entering a deep fade for longer than some specified period, especially when the vehicle moves at a low speed. The exact choice of these will depend on the fading rate, and the switching threshold.

REFERENCES

1. Young, W.R. Jr, and Lacy, L.Y. "Echoes in Transmission at 450 Megacycles from Land-to-Car Radio Units", IRE Proc., Vol. 38, pp. 255-258, 1950.

2. Cox, D.C. "910 MHz Urban Mobile Radio Propagation: Multipath Characteristics in New York City", IEEE Trans., Vol. VT-22, pp. 104-110, 1973.

3. Young, W.R. Jr. "Comparison of Mobile Radio Transmission at 150, 450, 900 and 3700 MHz", BSTJ, Vol. 31, pp. 1068-1085, 1952.

4. Reudink, D.O. "Properties of Mobile Radio Propagation above 400 MHz", IEEE Trans., Vol. VT-23, pp. 143-159, 1974.

5. Nylund, H.W. "Characteristics of Small-Area Signal Fading on Mobile Circuits in the 150 MHz Band", IEEE Trans., Vol. VT-17, pp. 24-30, 1968.

6. Clarke, R.H. " A Statistical Theory of Mobile-Radio Reception", BSTJ, Vol. 47, pp. 957-1000, 1968.

7. Meno, F.I. "Mobile Radio Fading in Scandinavian Terrain", IEEE Trans., Vol. VT-26, pp. 335-340, 1977.

8. Rustako, A.J. Jr. "A Mobile-Radio Space-Diversity Receiving System using Delta Modulation with STAR type Cophasing Scheme", IEEE Trans., Vol. VT-22, pp. 61-68, 1973.

9. Davis, B.R. "Random FM in Mobile Radio with Diversity", IEEE Trans., Vol. COM-19, pp. 1259-1267, 1971.

10. Clarke, R.H. "A Statistical Theory of Mobile Radio Reception", BSTJ, Vol. 47, pp. 957-1000, 1968.

11. Lee, W.C.Y. "Antenna Spacing Requirement for a Mobile Radio Base Station Diversity", BSTJ, Vol. 50, pp. 1859-1876, 1971.

12. Brennan, D.G. "Linear Diversity Combining Techniques", IRE Proc., Vol. 47, pp. 1075-1102, 1959.

13. Rustako, A.J. Jr., Yeh, Y.S. and Murray, R.R. "Performance of Feedback and Switch Space Diversity 900 MHz FM Mobile-Radio Systems with Rayleigh Fading", IEEE Trans., Vol. VT-22, pp. 173-184, 1973.

14. Shortall, W.E. "A Switched Diversity Receiving System for Mobile Radio", IEEE Trans., Vol. VT-22, pp. 185-191, 1973.

15. Parsons, J.D., Ratliff, P.A., Henze, M. and Withers, M.J. "Single Receiver Diversity Systems",IEEE Trans., Vol. VT-22, pp. 192-196, 1973.

16. Langseth, R.E. "On the Use of Space Diversity in the Square-Law Reception of Fading on-off Keyed Signals", IEEE Trans., Vol. VT-22, pp. 68-77, 1973.

17. Jakes, W.C. Jr. "A Comparison of Specific Space Diversity Techniques for Reduction of Fast Fading in UHF Mobile-Radio Systems", IEEE Trans., Vol. VT-20, pp. 81-92, 1971.

18. Rustako, A.J. Jr. "Evaluation of a Mobile Radio Multiple Channel Diversity Receiver Using Predetection Combining", IEEE Trans., Vol. VT-16, pp. 46-57, 1967.

19. Black, D.M., Kopel, P.S. and Novy, R.J. "An Experimental UHF Dual-Diversity Receiver Using a Predetection Combining System", IEEE Trans., Vol. VC-15, pp. 41-47, 1966.

20. Gans, M.J. "A Power-Spectral Theory of Propagation in the Mobile Radio Environment", IEEE Trans., Vol. VT-21, pp. 27-38, 1972.

21. Rice, S.O. "Statistical Properties of a Sine Wave Plus Random Noise", BSTJ, Vol. 27, pp. 109-157, 1948.

22. Cox, D.C. "Time- and Frequency-Domain Characterizations of Multipath Propagation at 910 MHz in a Suburban Mobile-Radio Environment", Radio Science, Vol. 7, pp. 1069-1077, 1972.

23. Davis, B.R. "FM Noise with Fading Channels and Diversity", IEEE Trans., Vol. COM-19, pp. 1189-1200, 1971.

24. Staras, H. "Diversity Reception with Correlated Signals", Journal of Applied Physics, Vol. 27, pp. 93-94, 1956.

25. Packard, K.S. "Effect of Correlation on Combiner Diversity", IRE Proc., Vol. 46, pp. 362-363, 1958.

26. Lee, C.Y. and Yeh, Y.S. "Polarization Diversity System for Mobile Radio", IEEE Trans., Vol. COM-20, pp. 912-923, 1972.

27. Schwartz, M., Bennett, W.R. and Stein, S. "Communications Systems and Techniques", New York, McGraw-Hill, 1965.

28. Parsons, J.D., Henze, M., Ratliff, P.A. and Withers, M.J. "Diversity Techniques for Mobile Radio Reception", The Radio and Electronic Engineer, Vol. 45, pp. 357-367, 1975.

29. Jakes, W.C. Jr. "New Techniques for Mobile Radio", Bell Lab. Record, pp. 326-330, 1970.

30. Davis, B.R. "A Fading Simulator", Research Report No. 3/75, Dept. of Elec. Eng., University of Adelaide.

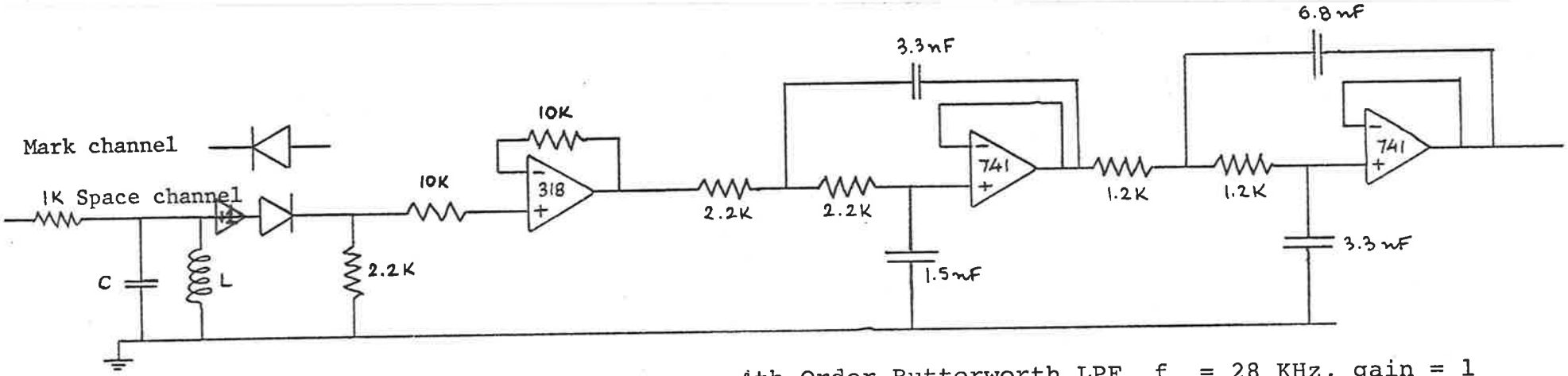


4th Order Butterworth LPF, $f_c$ = 28 KHz, gain = 1

Mark channel: $f_o$ = 1.1 MHz, gain ≈ 0.7

C = 2.7 μF, L = 7.75 μH

Space channel: $f_o$ = 0.9 MHz, gain ≈ 0.7

C = 2.7 μF, L = 11.58 μH

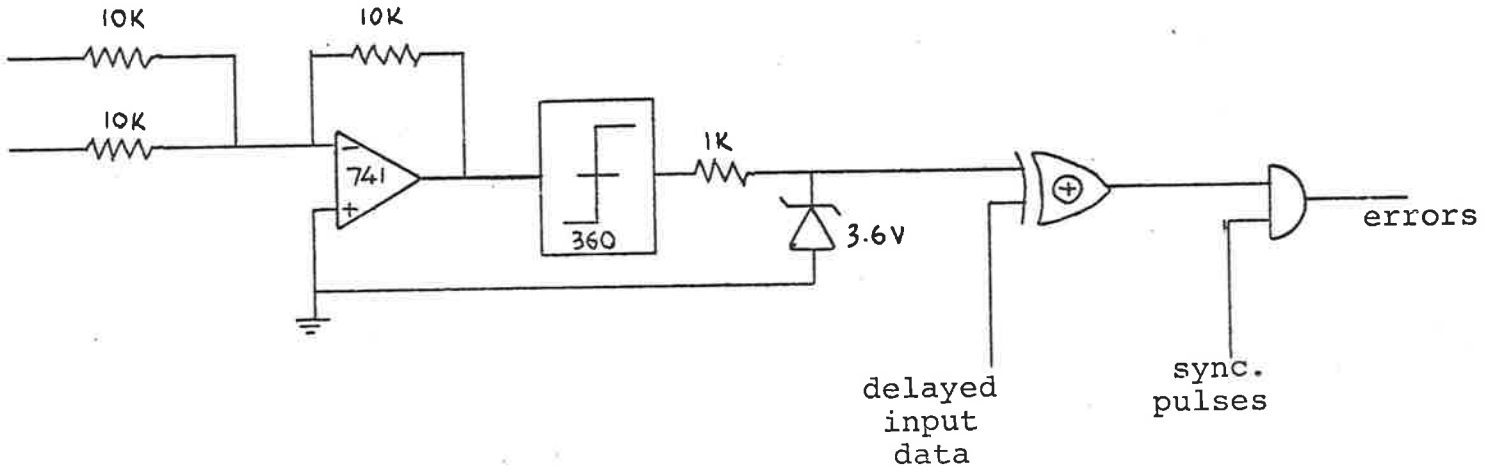

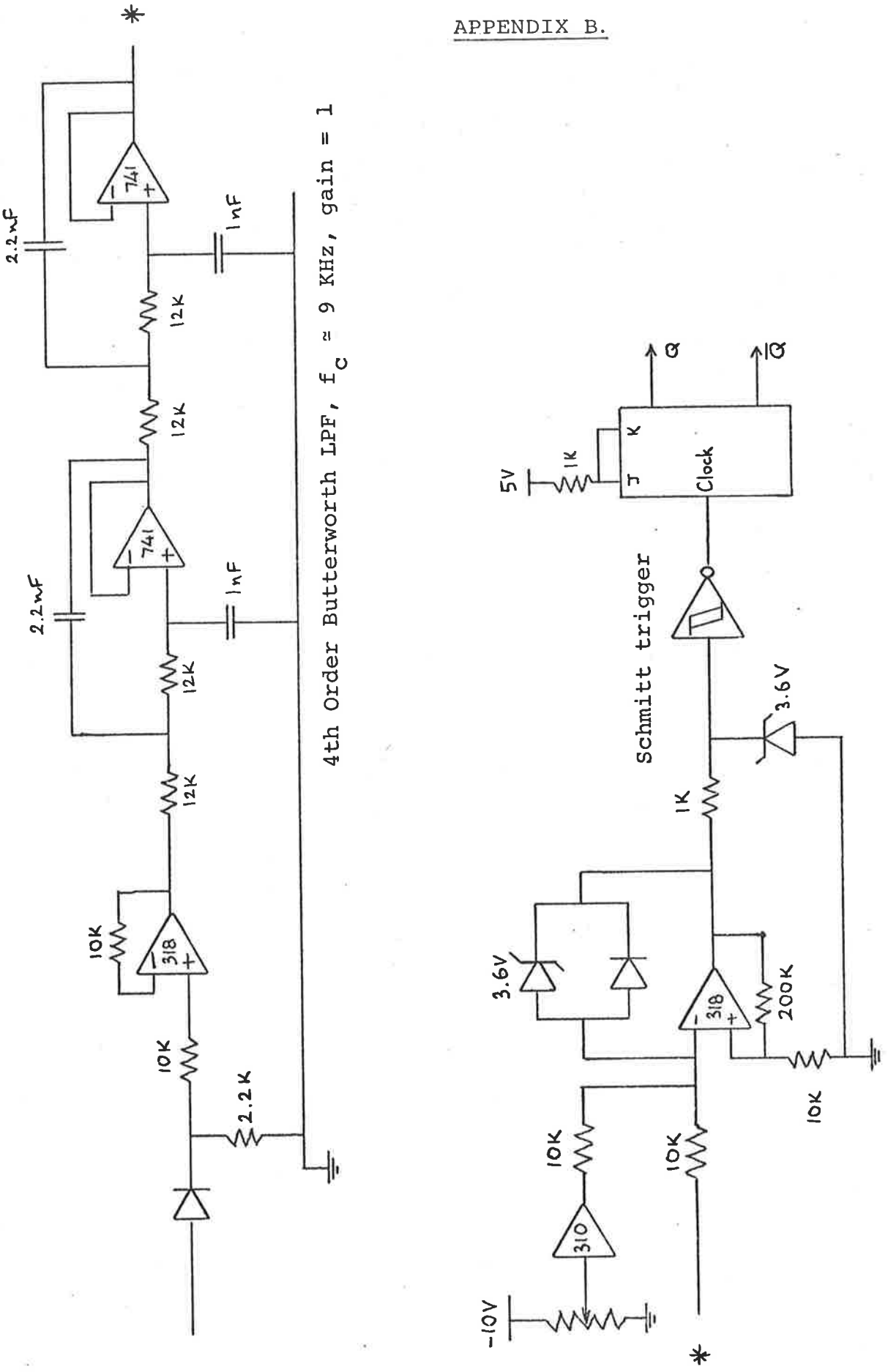


FADE DETECTOR

# APPENDIX C.

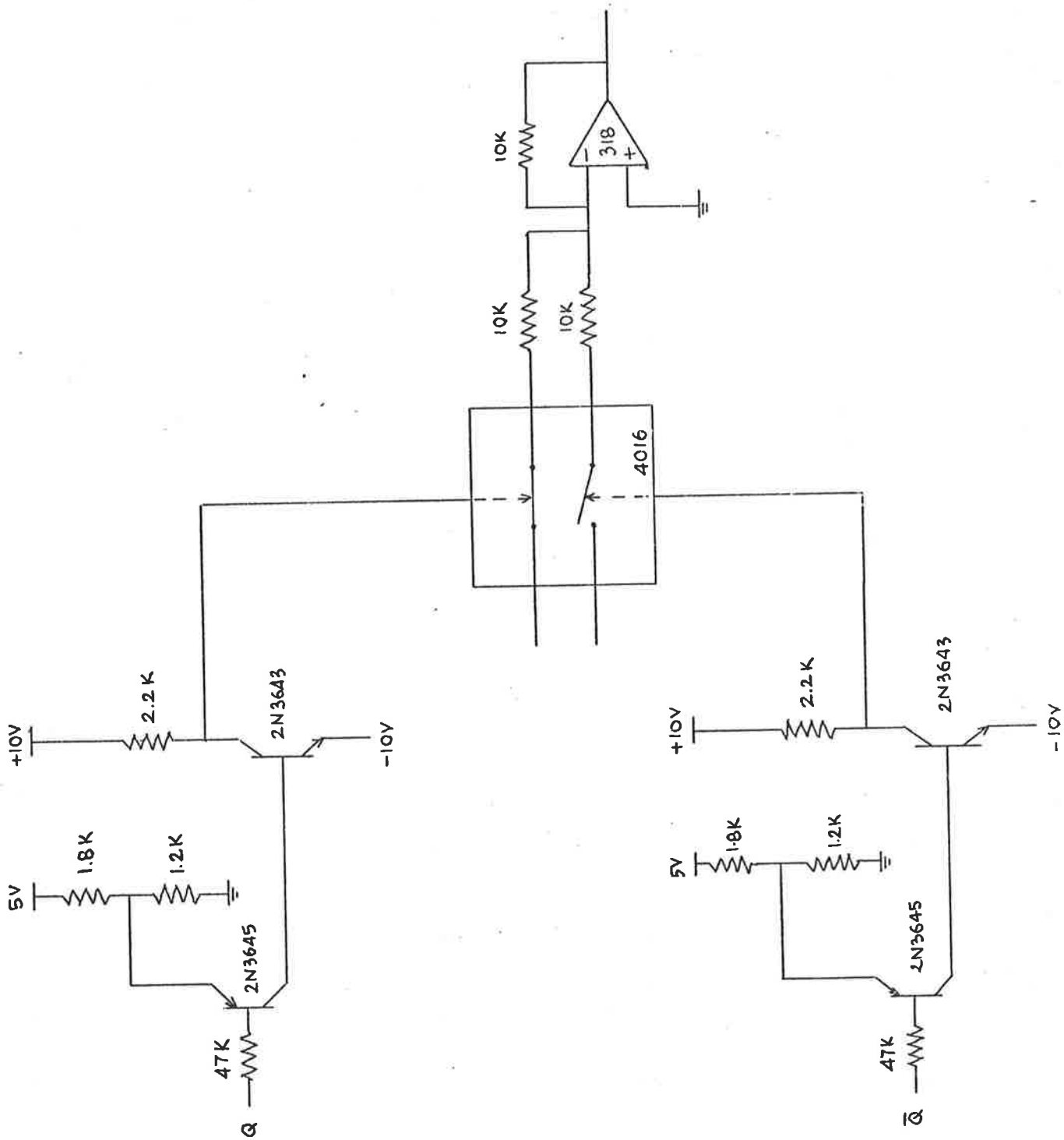


SWITCH